POLITECNICO DI TORINO

Master degree course in Mechanical Engineering

Experimental Analysis of a Geothermal Heat Pump.

Master's degree thesis

Supervisor:

Davide Papurello Ph.D.

Candidate:

Musurmonov Madumar

Torino 2021

Contents

List of figures

List of tables

Introduction

Nowadays, the demand for renewable energy sources is intensifying because of dangerous aspects of using fossil fuels such as gas, oil, and coal that derive great problems of global warming. Since the industrial revolution, man has begun to produce energy using hydrocarbons and resulting in the emission of greenhouse gases that capture atmospheric heat causing a series of changes in climatic conditions and damaging most types of living species. Starting from the awareness of this serious problem, some objectives were set with the Kyoto protocol (1997), starting an energy policy based on the reduction of these emissions: by 2020 we intend to reduce the production of greenhouse gases by 20% compared to 1990 emissions. For this reason, in the mechanical and energy fields, the creation of machines that allow reducing consumption to a minimum is becoming increasingly important, optimize the operation and, in some cases, even delocalize the inevitable emissions of pollutants, produced for example by combustion.

Geothermal energy is one of the most promising among renewable energy sources and its importance is increasing worldwide and already it has proven to be reliable, safe, and clean and therefore, its use for power production and heating and cooling is among many developed countries because it is a power source that produces electricity with minimal environmental impact.

A heat pump that uses geothermal energy is useful for obtaining these results: it uses clean and free geothermal energy, coming from the great thermal inertia of the ground, and uses electricity. The production of electricity can derive from renewable sources,

This thesis aims to describe and contextualize the use of a machine such as a closed-circuit geothermal heat pump, and the reasons why it is preferable in some cases, especially concerning a more common boiler heating system. The results obtained from the study will be dealt with more technically. From the outset, the analysis carried out had the objectives of quantifying the efficiencies and energy quantities involved during the operation of the Nibe F1155 6kW heat pump installed at the Energy Center. Data obtained through the sensors inside the machine itself, which worked in heating or cooling mode, were used, with which the COPs were then calculated using a spreadsheet. In parallel, we will calculate the results by using Coolpack software, and finally, we can make a decision

working efficiency of the system by comparing experimental and simulative results.

Initially, during Chapter 1, we will give some brief explanation about renewable energy sources and general concepts on geothermal energy, its advantages, coverage in the world, species according to purpose.

Chapter 2 is entirely dedicated to the brief explanation of a Geothermal Heat Pump System. Starting from the resource, it is proposed the classifications of Closed-loop and Open-loop geothermal connections, their relative characteristics, and all possible shapes and conformations. A brief description of heat pump technology is present.

In chapter 3 we will show some characteristics of the NIBE1155 6kW heat pump in a detailed way. Technical data, working conditions, installation diagrams will be provided.

The case study of this thesis is described in Chapter 4, we will compare the results which is calculated from the available data, and the results obtained by inserting the same data into the Coolpack software, to understand if there are actual problems at the operating level that preclude the use. of a heat pump of this type in a residential environment. And will try to optimize the working condition of the pump if obtained results are unreal, and finally making some conclusions.

Chapter 1 Geothermal energy

1.1 Renewable energy sources.

Today in the world one of the biggest problems is global warming and the greenhouse effect. The main reasons are fossil fuels that emit carbon dioxide and a great number of greenhouse gases that hazardous for climate, air quality, the health of lives in the world, etc. Fossil fuels can contribute sulfur emission to the atmosphere as acid rains which can damage buildings and plants. And also these kinds of traditional energy sources are limited and they can't be renewable. In the last few decades, world scientists are trying to reduce air pollution and global warming causes. For that, the demand for renewable and energy-saving resources is increasing in many countries.

What is renewable energy?

"Renewable energy is energy derived from natural resources that replenish themselves in less than a human lifetime without depleting the planet's resources. These resources – such as sunlight, wind, rain, tides, waves, biomass, and thermal energy stored in the earth's crust (geothermal) – are available in one form or another nearly everywhere. They are virtually inexhaustible. And, what is even more important, they cause little climate or environmental damage."[1] (REN21, 2021)

Today, the world is still heavily dependent on fossil fuels and even continues to subsidize them. Meanwhile, the pollution they cause, from climate-damaging greenhouse gases to health-damaging particles, has reached record levels. And when something goes wrong, for example, when the Deepwater Horizon oil rig exploded in 2010, the consequences are dramatic. Since 2011, renewable energies have developed faster than all other forms of energy. Renewable energy had another record year in 2020, with installed electric capacity increasing by more than 256 gigawatts (GW), its largest increase to date. Over 29% of our electricity now comes from renewables, and this continues to grow

[1] https://www.ren21.net/why-is-renewable-energy-important/

Despite the impacts of the COVID-19 pandemic, renewables set a record for new energy capacity in 2020 and were the only source of power generation to record a net increase in total capacity. Investment in renewable energy capacity increased, albeit slightly, for the third year in a row, and companies continued to set records for renewable electricity supply. More and more countries have turned to renewable energies for the electrification of heat. Although the production of biofuels for transportation has declined, sales of electric vehicles (EVs) have increased, as has the coupling of electric vehicles and renewables, albeit to a lesser extent. China has been one of the countries that have stepped up its commitments to act on the climate crisis by establishing a carbon-neutral target. The United States joined the Paris Agreement in early 2021. (Global Status Report GSR21)

Renewable energy sources play an important role in the construction of heating and cooling systems. Figure 1 shows the latest data available for the share of renewables in gross final energy consumption and the targets that have been set for 2020.

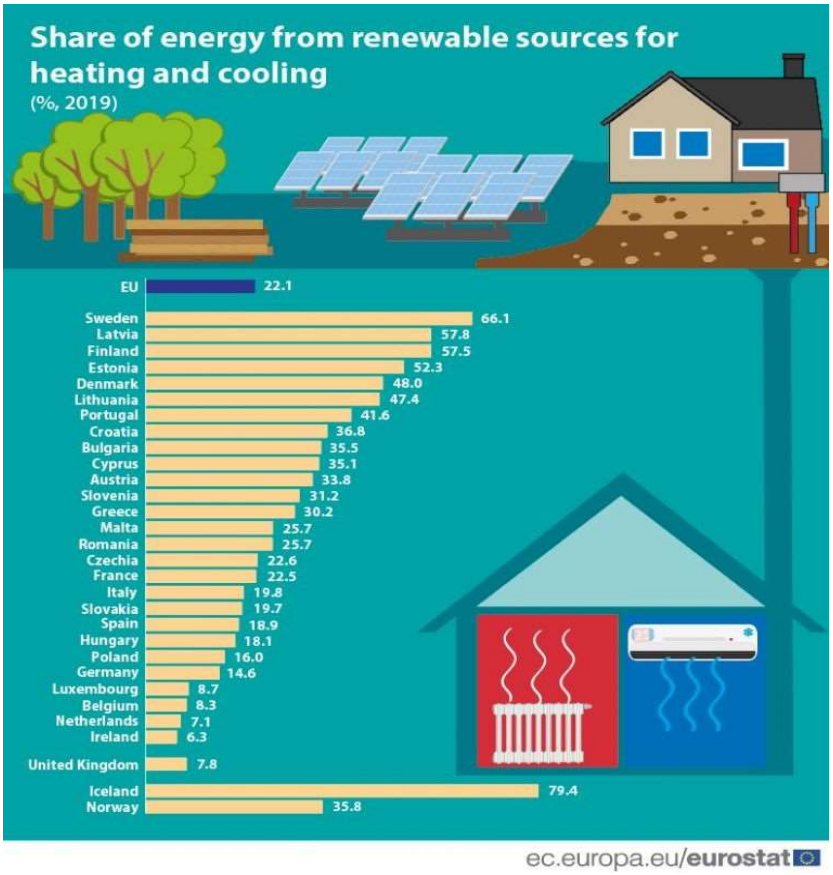

Figure 1: Renewable energy for heating and cooling 2019

Right across Italy and overseas, Green Network Group develops electricity production plants fueled by renewable sources: photovoltaic, wind energy, biomass. In figure 2 you can see the evolution of production from renewable sources in 2016. over Italy.

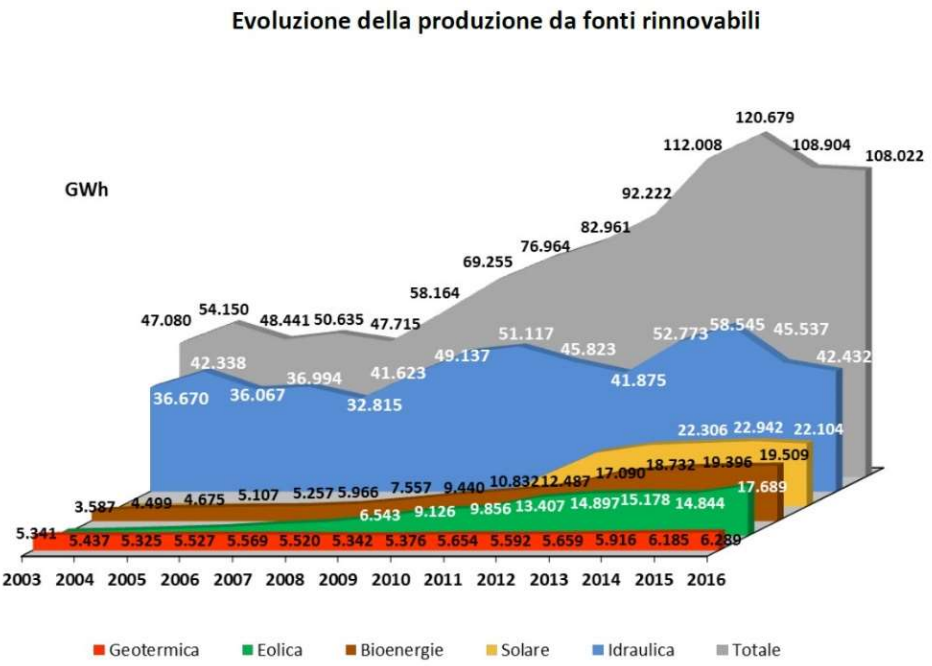

Figure 2: The evolution of production from renewable sources in 2016

What are the advantages of renewable energy?

1) It is considered clean energy that doesn't cause grave air pollution because of low or zero carbon dioxide
2) It is renewable as it called since this kind of energy doesn't deplete over a lifetime and almost impossible to run out in the future (sustainable energy source)
3) Renewable energy technologies require less overall maintenance. Only installation is required.
4) Renewable energy saves money in the long run. You will not only save on maintenance costs but also operating costs. And there are many advantages.

Even they have some drawbacks like low efficiency, low capacity, large space to install, relatively high initial instalment cost, expensive storage for energy, and weather dependent (wind and sunny days) we have to change our current energy sources that are harmful to our earth's future to eco-friendly and renewable energy types.

1.2 Geothermal energy

Geothermal energy, one of the most promising renewable energy sources, is reliable, safe, and clean, and as a result, its use for power generation, cooling, and heating is expanding rapidly. Geothermal energy is an energy source that produces electricity with minimal environmental impact (Fridleifsson, 2001; Barbier, 1997). Geothermal energy has been produced commercially for about 90 years and four decades at the scale of hundreds of MW for power generation and direct uses. Most of the world's geothermal power plants were built in the 1970s and 1980s after the 1973 oil crisis. Different authors have made different estimates of the geothermal potential for power generation and direct uses. The world's geothermal potential for generating electricity is expected to be between 35 and 72 GW. With improved technology, such as improved permeability, improvements in drilling, this range could reach up to 138 GW (Bahtiyar Dursun, 2011)

Geothermal energy, around the world, is used in various forms, such as space heating and domestic hot water supply, CO2 and dry ice production, greenhouse heating, balneology, water pumps. land heat and power generation.

"Geothermal energy is the energy contained within the high-temperature mass of the Earth's crust, mantle, and core. Since the Earth's interior is much hotter than its surface, energy flows continuously from the deep, hot interior up to the surface. This is the so-called terrestrial heat flow. The temperature of the Earth's crust increases with depth following Fourier's law of heat conduction. Thus the energy content of a unit of mass also increases with depth."[2] (Aniko Toth, 2017,)

Geothermal energy is produced by exploiting the energy of the heat in the deepest layers of the Earth's crust. It is obtained by channelling the steam deriving from the subsoil into turbines which are used to produce electricity and by recycling the water vapour produced to heat buildings, for greenhouses, and various uses in heating systems.

The first Italian plants for the production of geothermal energy date back to the beginning of the 20th century and today most are concentrated in Tuscany, with a potential of over 4 billion kWh only in the plants of Larderello (PI) and Montieri. Larderello was the site of the world's first geothermal power station,

[2] Aniko Toth, Elemer Bobok, "Flow and heat transfer in geothermal systems" 2017, page 1

built-in 1904, and the first geothermal power station in 1913. The town is also home to the Geothermal Museum (Geothermal energy, n.d.).

Here we can see that how geothermal energy utilization is increasing year by year over the world, and also it's shown the 8 main spheres of geothermal energy consumption. This information was for 2015, but nowadays these numbers have been getting doubled or more

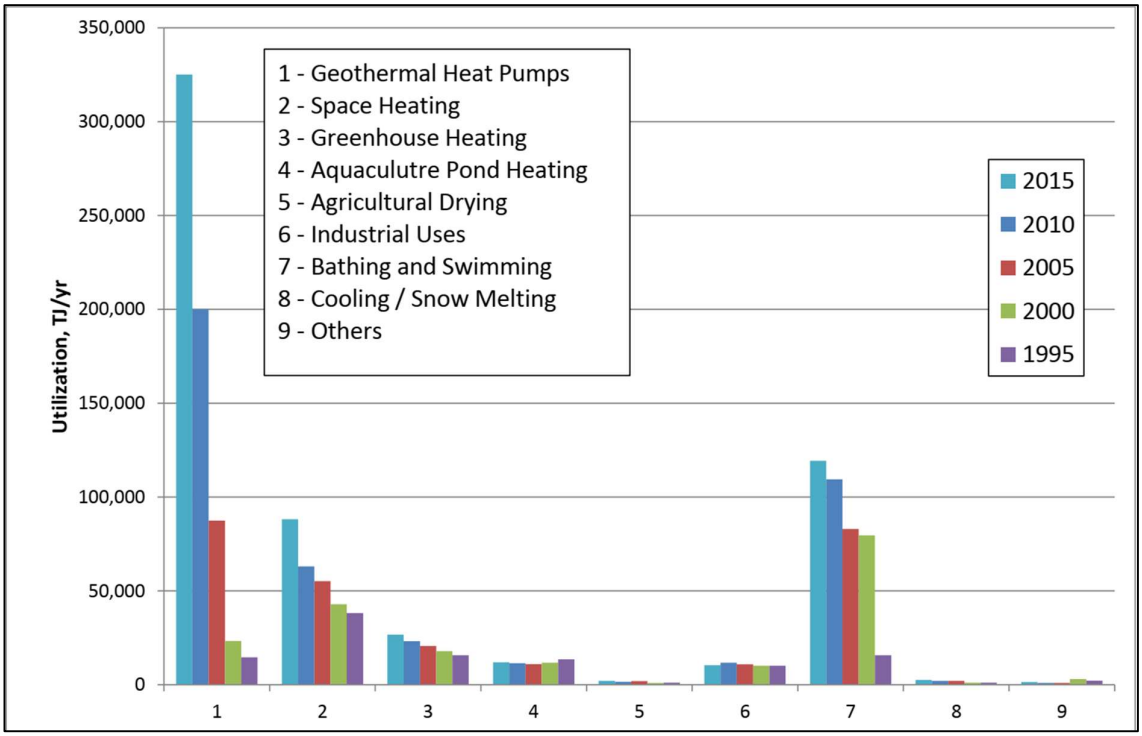

Figure 3 Installed capacity of the utilization of geothermal energy estimation in the world.

Important advantages of geothermal energy:

1) Geothermal energy is called renewable and sustainable because of the heat that the earth produces for millions of years and because after transporting hot water or steam through the ground, its heat is used for different purposes, and during the process, heat is formed water of the fluid is injected into the earth, so it will not diminish like fossil fuel reserves.

2) Geothermal energy provides a clean, renewable energy source that could dramatically improve our environment. Geothermal energy can make an important contribution to reducing atmospheric emissions from fossil fuels and also to offsetting atmospheric emissions from fossil fuel-fired power plants. It is

obvious that geothermal energy, whose gas emissions are low (most likely negligible compared to gas emissions from coal), easily qualifies as environmentally friendly. (Bahtiyar Dursun, 2011)

Three main applications of geothermal energy should be distinguished: high, medium, and low enthalpy systems. For geothermal high enthalpy or deep Geothermal, we mean that area of geothermal energy that exploits the heat coming from hot fluids, such as hydrothermal systems. In these plants, located at depths ranging from tens of meters to several kilometres, the temperatures are very high, from 150 °C to 350 ° C and the heat is converted into electricity by turbogenerators. Instead, we talk about geothermal low enthalpy or surface geothermal to indicate that branch of geothermal energy that exploits the heat coming from the surface layer of the soil, up to a depth of 100-200 m generally characterized by a temperature below 40 °C.

Having the geothermal energy at various temperatures, a classification of the resources is necessary. In the past, considering the temperature of the resource, some of the famous researchers distinguished three enthalpy levels using different temperature thresholds, this is notable in the table below. (M.H. Dickson, 1990)

	Muffler and Cataldi (1978)	Hochstein (1990)	Benderitter and Cormy (1990)	Nicholson (1993)	Axelsson and Gunnlaugsson (2000)
Low Enthalpy resources	< 90	< 150	< 100	≤ 150	≤ 190
Intermediate Enthalpy resources	90 ÷ 150	125 ÷ 225	100 ÷ 200	-	-
High Enthalpy resources	> 150	> 225	> 200	> 150	> 190

Figure 4 Classification of Geothermal resources by temperature level [°C]

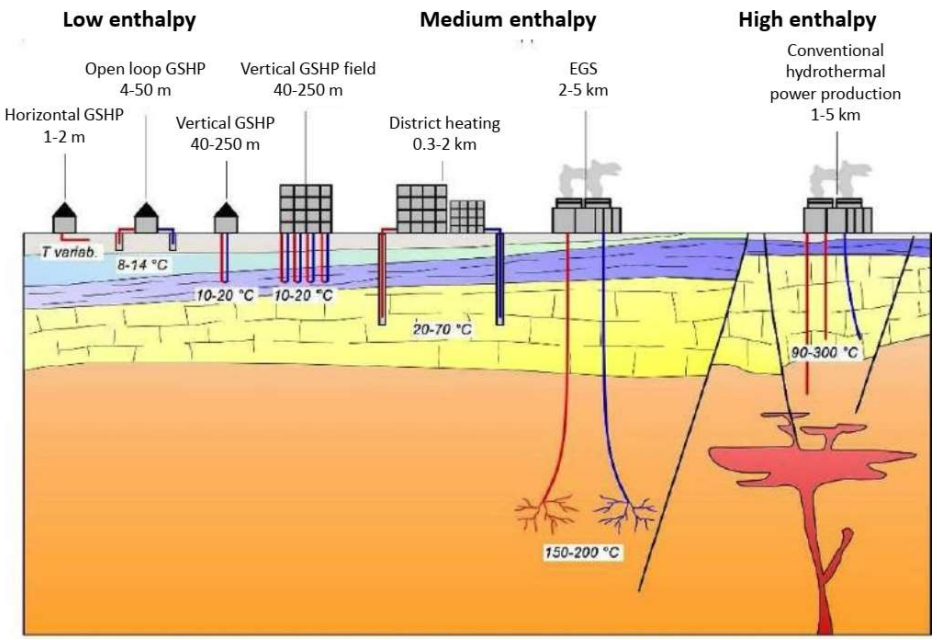

Figure 5 types of energy applications according to enthalpy level (Manzella)

In Italy the ground has a constant temperature of 12 ° -14 ° C from 10m to 100m which increases with depth according to the characteristics of the subsoil and the presence of water: there is an increase of 3 °C per 100m depth of soil. In the figure below it is possible to observe the trend of the soil temperature during the winter and summer months according to the depth.

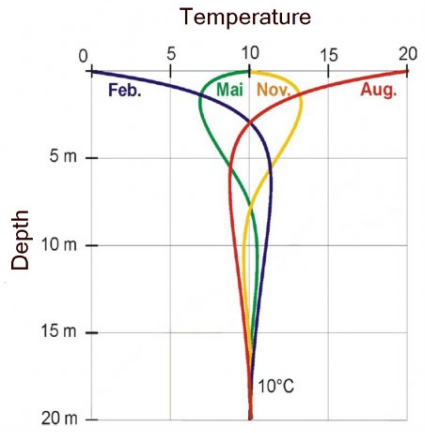

Figure 6 Diagram of the subsoil Temperature according to the depth of soil layer (Rivas, 2020)

Chapter 2 Geothermal heat pumps

Geothermal heat pumps (GHP) are one of the fastest-growing applications of renewable energy in the world, with annual increases of 10% in about 30 countries over the past 10 years. Its main advantage is that it uses normal ground or groundwater temperatures (between about 5 and 30), which are available in all countries of the world. The present worldwide installed capacity is estimated at almost 12,000 MWt (thermal) and the annual energy use is about 72,000 TJ (20,000 GWh). The actual number of installed units is around 1,100,000, but the data are incomplete.

GSHP can reduce energy consumption, and corresponding air pollution, by up to 44% compared to air-source heat pumps and up to 72% compared to electric resistance heating with traditional air conditioning equipment. (Source: EPA, 1993)

GHPs use the earth's relatively constant temperature to provide heating, cooling, and domestic hot water for homes, schools, government, and commercial buildings. A small amount of electricity is needed to run a compressor; however, energy production is on the order of four times this input. These “machines” circulate heat “upstream” from a lower temperature location to a higher location, in effect nothing more than a refrigeration unit that can be reversed. "Pump" is used to describe the work being done, and the temperature difference is called "lift" - the higher the lift, the greater the energy input. The technology is not new, as Lord Kelvin developed the concept in 1852, which was later modified as GHP by Robert Webber in the 1940s. They gained commercial popularity in the 1960s and 1970s. (J. Lund1, 2004)

2.1The operation principles of GSHP

The operation of the machine is cyclical and is based on four main transformations: evaporation, compression, condensation, and expansion. The refrigerant fluid present inside the circuit is heated using a geothermal heat source and when it reaches the boiling point, it evaporates. Inside the compressor which is the active part of the system, the gaseous fluid undergoes an increase in pressure and a further increase in temperature used to heat the rooms of the building. This heat exchange causes the passage of state from gas to liquid inside the condenser as the fluid decreases its temperature while maintaining still high pressure. (Tofalo, tesi "Sperimentazione di muri energetici", 2019)

In most cases, geothermal heat pump systems have a double role in space conditioning. During the cold seasons, these systems are used to heat the spaces, in particular, heat pumps bring an amount of heat from the geothermal resource to the thermal user. In figure 6 the scheme of the heating cycle GHP system is shown. On the opposite, during hot seasons geothermal heat pump systems can extract heat from the thermal users to carry it to the geothermal resource which, in this case, is considered as a thermal sink. In this way, the geothermal resource can be accounted as a tank of energy rather than a pure source of heat. (Figure 7)

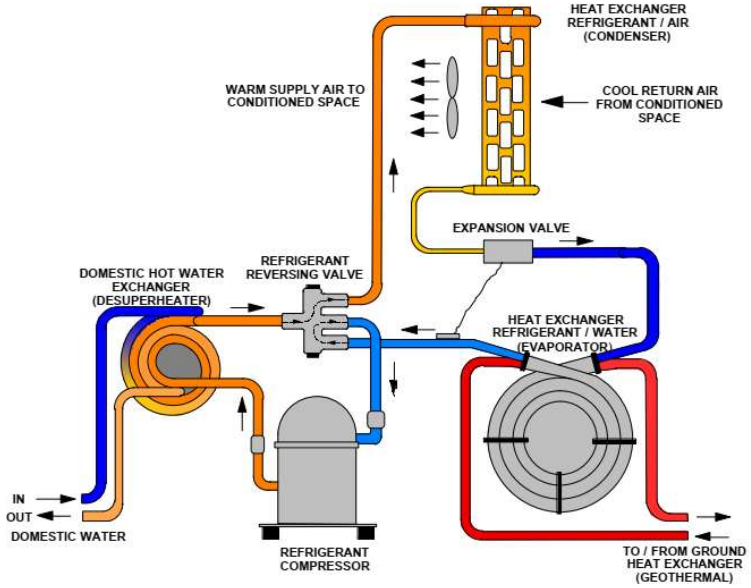

Figure 7. GHP in the heating cycle (source: Oklahoma State University).

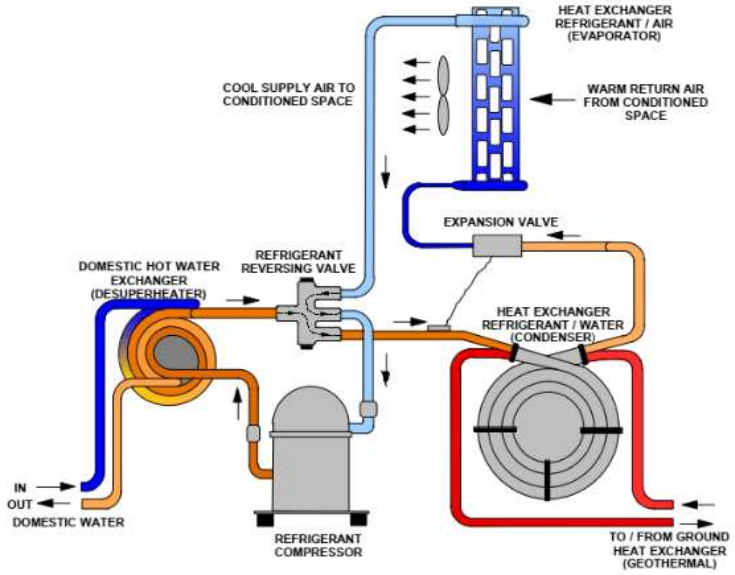

Figure 8 GHP in the cooling cycle (source: Oklahoma State University).

The refrigerant fluid must be chosen according to the condensation and evaporation pressure which must be moderate, the heat of vaporization which must be high, and the specific volume of the saturated vapour which must be as low as possible to minimize the volumetric flow rate. For the choice of the refrigerant fluid, it is necessary to opt for a substance that does not damage the stratospheric ozone, as established by the Montreal Protocol, therefore that it has a reduced content of chlorine and fluorine to minimize the impact on the environment, as highlighted by the Kyoto Protocol, also avoiding flammability problems.

The efficiency of the GSHP system is described by the COP (coefficient of performance) in the heating mode and the EER (energy efficiency ratio) in the cooling mode which is the ratio of the output energy divided by input energy which is the electricity consumed by the compressor pump and this COP varies from 3 to 6 with present equipment Thus, if COP is 4, then it would indicate that the unit produced 4 units of heating energy for every unit of electrical energy input. (J. Lund1, 2004)

Higher COP means the lower external energy input compared to useful heat because COP depends on the heat pump itself and the temperature difference between the cold and hot sides (see figure 9). For the heat pump under defined temperature conditions COP can be given, or as an annual COP which is called SPF (Course_GT)

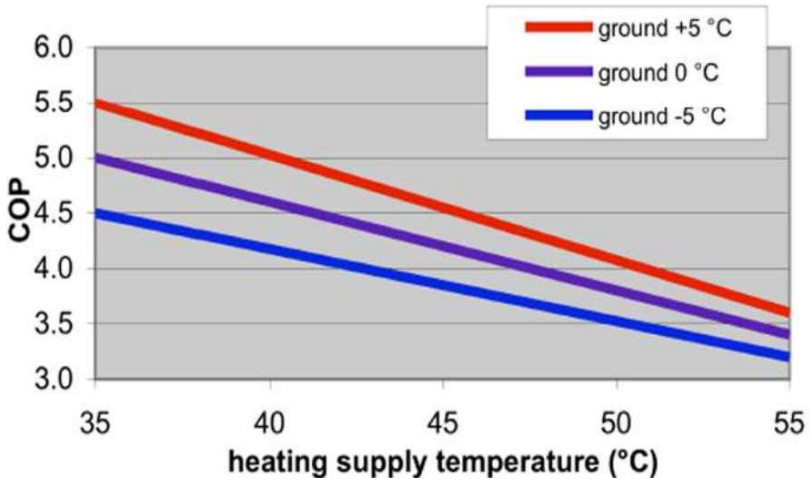

Figure 9 COP according to space heating supply temperature (Course_GT)

2.2 Types of geothermal heat pumps

Geothermal heat pumps are involved four types of loop systems that loop heat to or from the ground and your house. Three of them – horizontal (1 to 2m deep), vertical (50 to 100m deep), and pond/lake – are closed-loop systems. The fourth type of system is the open-loop option. Choose the one that best suits its site depends on the climate, the soil conditions, available land, and Installation costs on site. (US, 2011)

2.2.1 Open-loop geothermal heat pumps

In open-loop GHPs there is a direct exchange between the heat pump and the heat transfer fluid represented by groundwater (aquifers) and surface waters (rivers, lakes, sea, and artificial basins) which are not available everywhere and whose use is subject to restrictions. and constraints dictated by local regulations. Surface water was used for the first time in 1940 for the air conditioning of a commercial building and gave way to the diffusion of the systems open loop, many of them in Italy. Thanks to the presence of two wells, one for extraction (or production) through which the water is extracted and an injection well-aimed at introducing the fluid that has undergone heat exchange, it is possible to exploit the surface water at 10 ° -15 °C or the underground one at 10 ° -12 °C. The injection can occur directly from a lake or river or it can occur within a single well along with the extraction mechanism. A particular open circuit system is represented by the standing column wells, whose operating principle is based on the use of a single well for withdrawal and reintroduction: in fact, the water is withdrawn from the bottom of the well and end of the heat exchange inside the heat pump is reintroduced in the upper part of the well as shown in figure 8. (Tofalo, tesi "Sperimentazione di muri energetici", 2019)

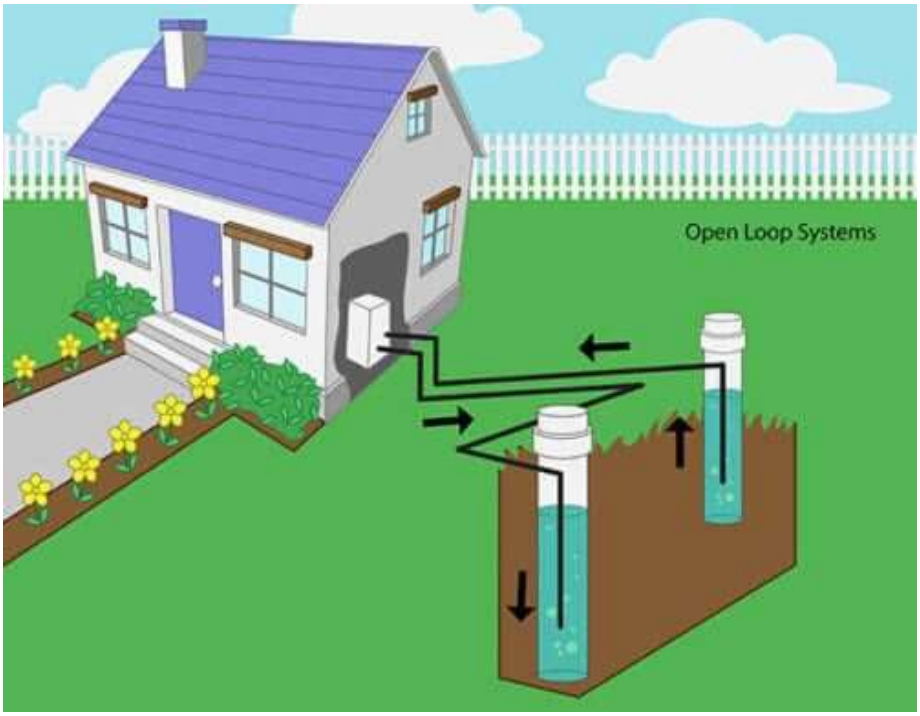

Figure 10 Open-loop geothermal heat pump system

The efficiency of the open-loop GHP system is much higher than closed-loop systems. Because heat exchange in wells is easier than in plastic tubes which are used in closed-loop systems.

2.2.2 Closed-loop geothermal heat pumps

It is a fact that the closed-loop GHP system is that uses plastic flexible pipes placed in the ground to circulate the suitable water-antifreeze solution. This water solution is low freezing temperature and with good conductivity characteristics, helps to use almost in all seasons and better heat exchange with the ground to help pumps to work better performances. Pipes are installed underground horizontally (1-2 m) or vertically(50-250m) (Manzella)

Closed-loop GHPs can be installed almost everywhere in the world and all types of geological formations.

According to the shape of heat exchangers, closed-loop GHPs are divided into 3 main types: horizontal, vertical, and pond/lake type installations.

1) Horizontal closed-loop geothermal heat pumps

In general, horizontal loop installations are the most cost-effective for small volume GHP systems, and particularly for the new installation, we need more

sufficient land area (we need approximately 25 square meters to draw 1kW energy). The thermal recharge for almost all horizontal GHP systems is provided by the solar radiation of the land surface.

In horizontal closed-loop systems, the pipes are laid in long trenches deeper than the frost line. Some possible pipe installation alternatives are straight parallel horizontals (Figure 11) Once the pipes are in place, the trenches are filled. These systems are based on the fact that the heat from the ground generated by solar radiation is transferred to the working fluid in the pipes. As in this case, the pipes are laid relatively close to the ground surface, these systems are not effective in areas with extreme climatic conditions, where closed vertical systems are preferred. (Meho Saša Kovačević, 2013)

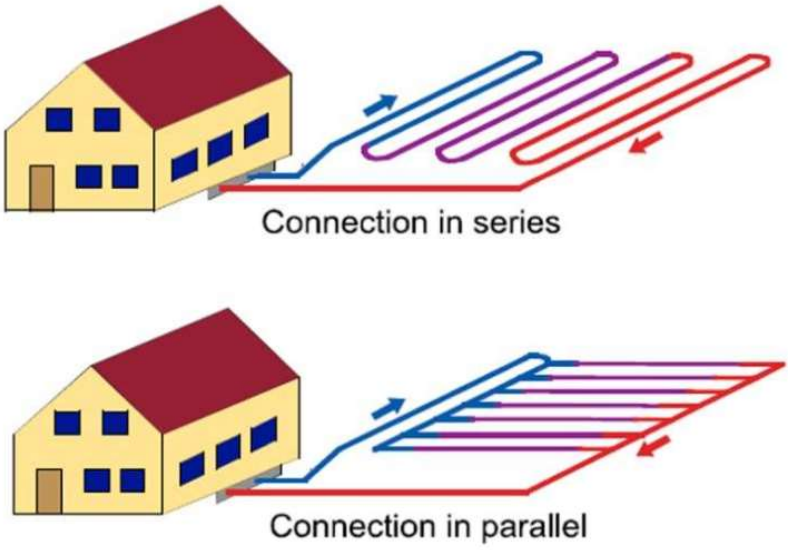

Figure 11 Horizontal closed-loop shallow GHP system (Course_GT)

2) Vertical closed-loop geothermal heat pumps

Vertical construction is more efficient than horizontal instalment if the areas are characterized by extreme temperatures, these kinds of systems are also favourable when the installation area of pipes is limited. Because we will drill the soil vertically and we don't need large space for that. Also, this would be useful when utilizing the geothermal potential of the rock in which this would be hard to excavate the ground for horizontal piping.

In the vertical installation, pipes are placed in vertical boreholes(GHE), and they will be one or several (figure 12). Commonly the depth of boreholes becomes

150-200m. Usually, three concepts of vertical piping are used: U-pipe, coaxial, and coil pipes

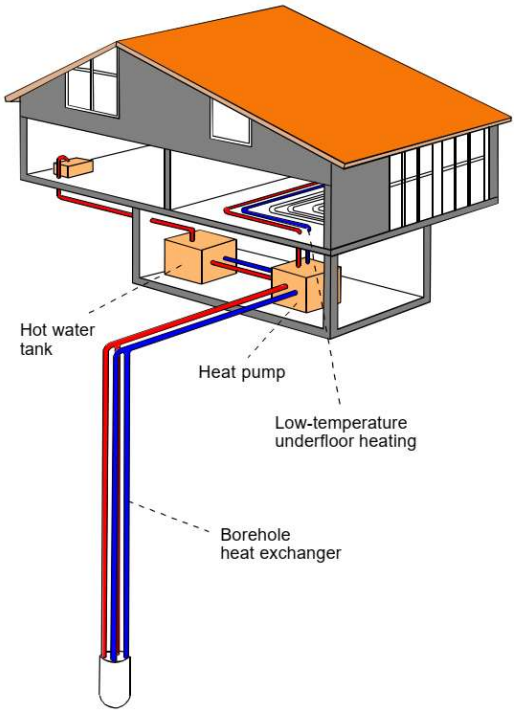

Figure 12 vertical closed-loop geothermal system (J. Lund1, 2004)

Because of the constant temperature of the soil in deeper points, the ground can provide building heating in the winter period and can cool down the building during summer days (figure 13)

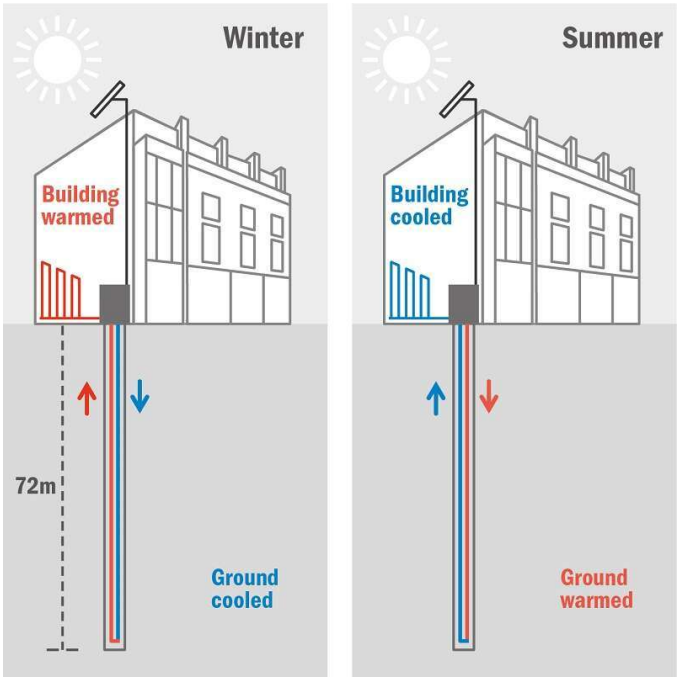

Figure 13 The cooling and heating mode of vertical loop GHP during seasons (IOP institute of physics, n.d.)

The space between the pipes and the well wall is filled with mud to ensure efficient heat transfer between the fluid in the pipes and the surrounding soil/rock. In addition, backfilling of boreholes is important because it prevents vertical entry of surface water and possible contamination of underground space. The thermal resistance of the borehole is very important in the process of heat transfer. It depends on the layout of the pipe in the well and the thermal properties of the grout used. The most commonly used grout mixes in this regard are cement-based or bentonite-based. Some studies have been carried out on the possible use of slurry mixtures based on fly ash, which is a by-product of industrial coal combustion. In addition, geothermal wells can also be filled with quartz sand. (Meho Saša Kovačević, 2013)

3) Pond/lake closed-loop geothermal heat pumps.

If there is surface water like a lake or river near a building, we can use a pond/lake loop system here, because this installation is the cheapest method. Closed-loop slinky coils are submerged in surface water at a depth of at least 2.5 m below the surface. Slinky coils are overlapping coils of polyethylene pipe which is effective on good heat exchange with water and usually, its length is relatively long (figure 14). (Course_GT)

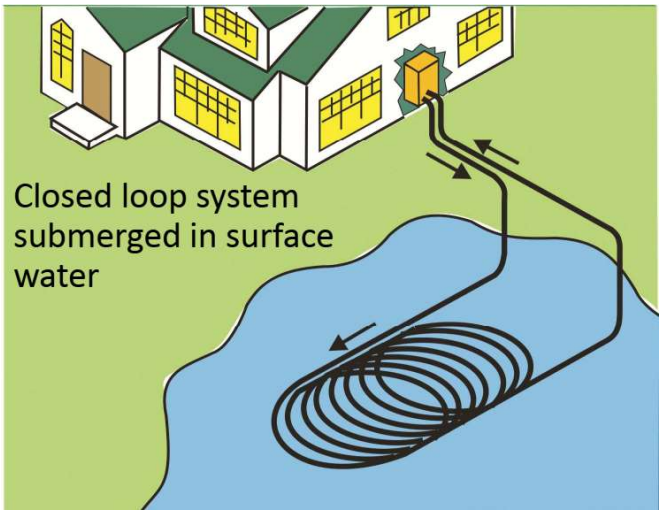

Figure 14 slinky loops are placed bottom of the pond. (Course_GT)

Chapter 3 Nibe F1155 (6kW, 1x230V)

In our thesis, we will analyze the working principles and characteristics of NIBE F1155 (figure 15). Because the energy center is equipped with NIBE F1155 geothermal pump which was installed on 19/07/2019 (GEONOVIS energia geotermica, 2019). This pump is an intelligent, inverter-controlled ground source heat pump without an integrated hot water tank, which makes it easy to install in locations with low ceilings. A separate hot water tank is selected according to hot water requirements. NIBE F1155 provides optimum savings since the heat pump automatically adapts to the building's heating demand.

Figure 15: NIBE heat pump of the center with a buffer tank and fan coil

This pump was installed after the completion of the construction of the energy center. That's why engineers faced some problems installing the geothermal pipes of the system, and it was so expensive to build and cost almost 30000 euros. This pump is a small system and just for experimental goals.

3.1 The technical characteristics of F1155

Before study and analyze the pump we will give some main technical characteristics of the NIBE GHP. There are 3 versions of NIBE F1155 according to its power 6 kW, 12 kW, and 16kW. Here we will focus on the 6 kW power version.

Rated voltage		*230V ~ 50Hz*
Rated output (PH)	kW	3.15
Supplied power (PE)	kW	0.67
COP		4.72
SCOPEN14825 cold climate 35 °C / 55 °C		5.5/4.1
SCOPEN14825 average climate, 35 °C / 55 °C		5.2/4.0
Efficiency class for space heating 35 °C /55 °C		*A++ / A++*
Space heating efficiency class of the system 35 °C / 55 °C1)		*A+++ / A+++*
Efficiency class hot water/charging profile with water heater		*A / XL* *VPB 300*
Sound power level (LWA) acc to EN 12102 at 0/35	dB(A)	36 – 43
Sound pressure level (LPA)calculated values according to EN ISO 11203 at 0/35 and 1m range	dB(A)	21 – 28
Output, Brine pump	W	10 – 87
Output, Heating medium pump	W	2 – 63
Enclosure class		IP21
Type of refrigerant		R407C
GWP refrigerant		1.774
Volume	kg	1.16
CO2 equivalent	ton	2.06
Cut-out value pressure switch HP / LP	MPa	3.2 (32 bar) / 0.15 (1.5 bar)
Difference pressure switch HP / LP	MPa	-0.7 (-7 bar) / 0.15 (1.5 bar)
Brine circuit		
Min/max system pressure brine	MPa	0.05 / 0.45
Nominal flow	l/s	0.18
Max external avail. press at nom flow	kPa	64
Min/Max incoming Brine temp	°C	see diagram
Min. outgoing brine temp.	°C	-12
Heating medium circuit		

Min/Max system pressure heating medium	MPa	0.05 / 0.45
Nominal flow	l/s	0.08
Max external avail. press at nom flow	kPa	69
Min/max HM-temp	°C	see diagram

Table 1: Technical specifications of F1155 (NIBE)

The working range heat pump and compressor operation

The compressor can provide a supply temperature up to 65 °C at 0 °C of incoming brine temperature. By using additional heat it is possible to take the remainder (up to 70 °C). Here we have some diagrams of the pump

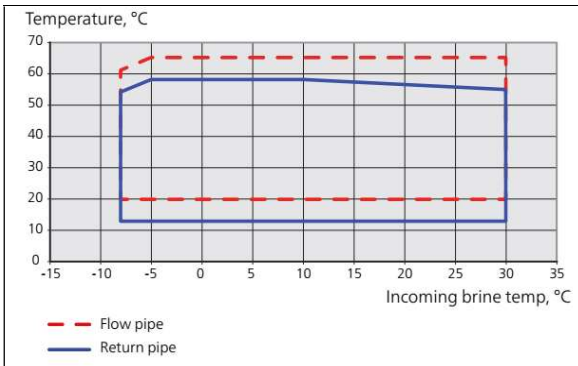

The working range below 75 %

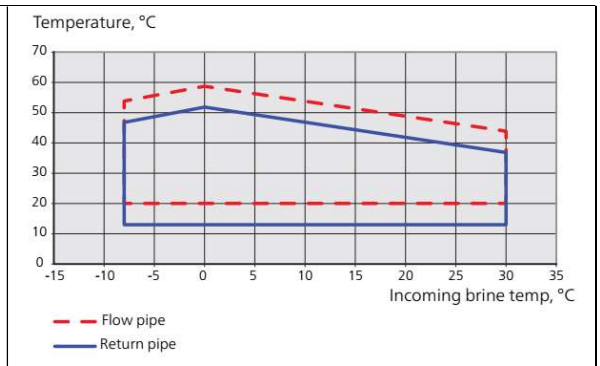

The working range above 75 %

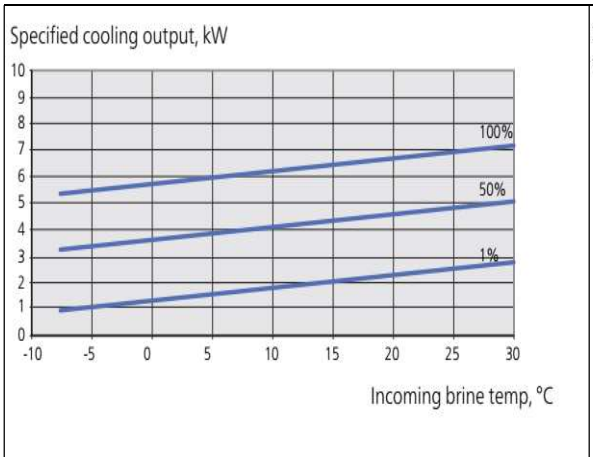

Supply temperature, heating medium 35 °C

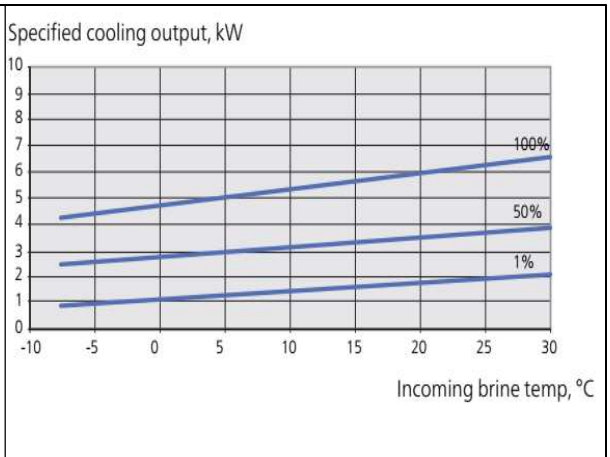

Supply temperature, heating medium 50 °C

Model		F1155-6 1x230V
Model hot water heater		VPB 300
Temperature application	°C	35 / 55
Declared load profile for water heating		XL
Seasonal space heating energy efficiency class, average climate		A++ / A++
Water heating energy efficiency class, average climate		A
Rated heat output (Pdesignh), average climate	kW	6
Annual energy consumption space heating, average climate	kWh	2,188 / 2,875
Annual energy consumption water heating, average climate	kWh	1,697
Seasonal space heating energy efficiency, average climate	%	200 / 150
Water heating energy efficiency, average climate	%	99
Sound power level L_{WA} indoors	dB	42
Rated heat output (Pdesignh), cold climate	kW	6
Rated heat output (Pdesignh), warm climate	kW	6
Annual energy consumption space heating, cold climate	kWh	2,481 / 3,287
Annual energy consumption water heating, cold climate	kWh	1,697
Annual energy consumption space heating, warm climate	kWh	1,408 / 1,852
Annual energy consumption water heating, warm climate	kWh	1,697
Seasonal space heating energy efficiency, cold climate	%	211 / 157
Water heating energy efficiency, cold climate	%	99
Seasonal space heating energy efficiency, warm climate	%	201 / 151
Water heating energy efficiency, warm climate	%	99
Sound power level L_{WA} outdoors	dB	-

Figure 16: Energy labelling information sheet (NIBE, NIBE F1155 Installer manual)

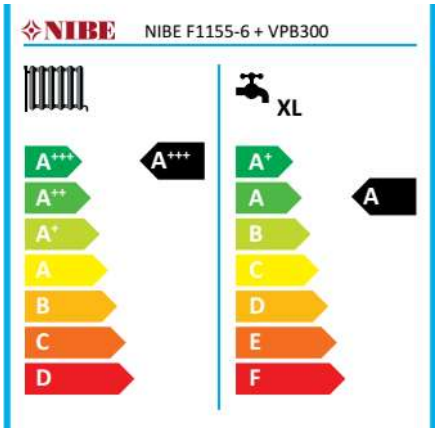

Model		F1155-6 1x230V					
Model hot water heater		**VPB 300**					
Type of heat pump		☐ Air-water ☐ Exhaust-water ☒ Brine-water ☐ Water-water					
Low-temperature heat pump		☐ Yes ☒ No					
Integrated immersion heater for additional heat		☒ Yes ☐ No					
Heat pump combination heater		☒ Yes ☐ No					
Climate		☒ Average ☐ Cold ☐ Warm					
Temperature application		☒ Average (55 °C) ☐ Low (35 °C)					
Applied standards		EN-14825 & EN-16147					
Rated heat output	Prated	5,5	kW	**Seasonal space heating energy efficiency**	η_s	150	%
Declared capacity for space heating at part load and at outdoor temperature Tj				*Declared coefficient of performance for space heating at part load and at outdoor temperature Tj*			
Tj = -7 °C	Pdh	5.0	kW	Tj = -7 °C	COPd	3.06	-
Tj = +2 °C	Pdh	3.0	kW	Tj = +2 °C	COPd	3.97	-
Tj = +7 °C	Pdh	2.0	kW	Tj = +7 °C	COPd	4.63	-
Tj = +12 °C	Pdh	1.2	kW	Tj = +12 °C	COPd	4.86	-
Tj = biv	Pdh	5.4	kW	Tj = biv	COPd	2.84	-
Tj = TOL	Pdh	5.4	kW	Tj = TOL	COPd	2.84	-
Tj = -15 °C (if TOL < -20 °C)	Pdh		kW	Tj = -15 °C (if TOL < -20 °C)	COPd		-
Bivalent temperature	T_{biv}	-10	°C	Min. outdoor air temperature	TOL	-10	°C
Cycling interval capacity	Pcych		kW	Cycling interval efficiency	COPcyc		-
Degradation coefficient	Cdh	0.99	-	Max supply temperature	WTOL	65	°C
Power consumption in modes other than active mode				*Additional heat*			
Off mode	P_{OFF}	0.002	kW	Rated heat output	Psup	0.1	kW
Thermostat-off mode	P_{TO}	0.007	kW				
Standby mode	P_{SB}	0.007	kW	Type of energy input	Electric		
Crankcase heater mode	P_{CK}	0.009	kW				
Other items							
Capacity control		Variable		Rated airflow (air-water)			m^3/h
Sound power level, indoors/outdoors	L_{WA}	42 / -	dB	Nominal heating medium flow			m^3/h
Annual energy consumption	Q_{HE}	2,875	kWh	Brine flow brine-water or water-water heat pumps		0.68	m^3/h
For heat pump combination heater							
Declared load profile for water heating		XL		**Water heating energy efficiency**	η_{wh}	99	%
Daily energy consumption	Q_{elec}	7.73	kWh	Daily fuel consumption	Q_{fuel}		kWh
Annual energy consumption	AEC	1,697	kWh	Annual fuel consumption	AFC		GJ

Figure 17: Technical documentation of the pump

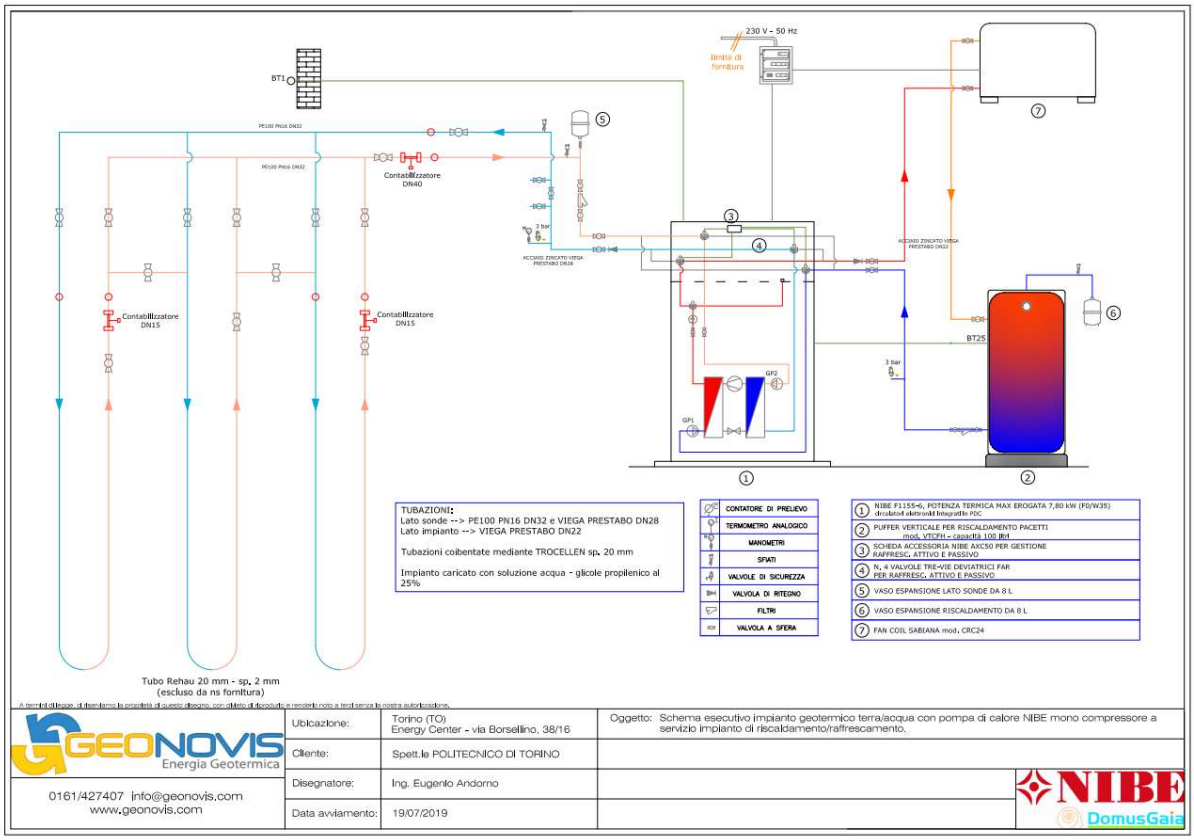

Figure 18 Plant project of the pump installed in the center (GEONOVIS energia geotermica, 2019)

3.2 Principle of operation

F1155 system contains a heat pump, immersion heater, circulation pumps, and control system. The pump is connected to the brine system and heating medium systems. And the whole system consists of 3 circuits: brine circuit, refrigerant circuit, and heating medium circuit (figure 19).

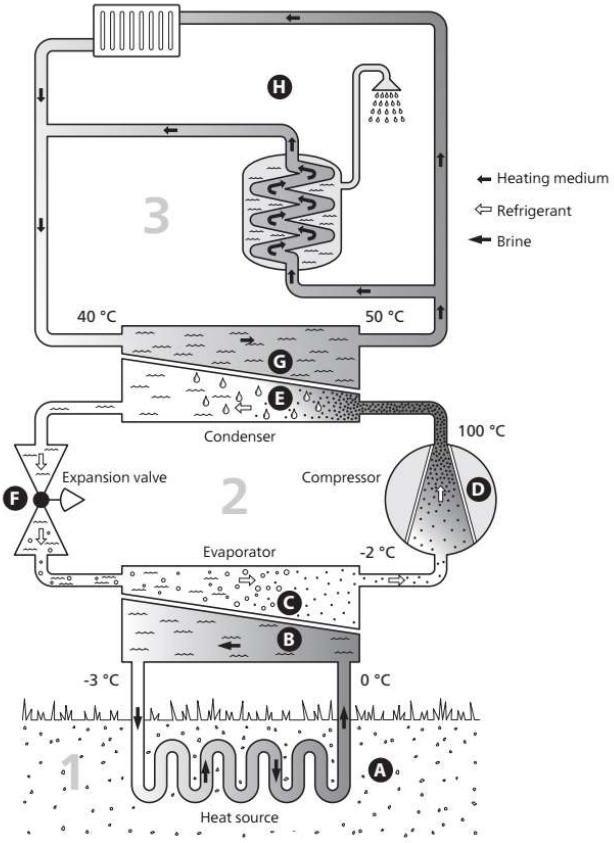

Figure 19: Scheme of the heat pump (The temperatures are only examples and may vary between different installations and times of the year.)

1) Brine circuit

A. This circuit provides the heat from the ground heat source (soil, rock pond) where the solar energy is stored. Heat transporting agent is brine which is water mixed with glycol, antifreeze, or ethanol. In our case, this mixture is 25% water solution propylene glycol that circulates in the highly flexible plastic pipes and gains energy from the ground. The probes are certified and have a diameter of 20mm and a thickness of 2.0mm. In the center, The wall extends for 7.50 m and reaches a depth of 4.6 m., three different pipe circuits with each one 2.5 m were installed, two horizontal and one vertical arrangement. (figure 20)

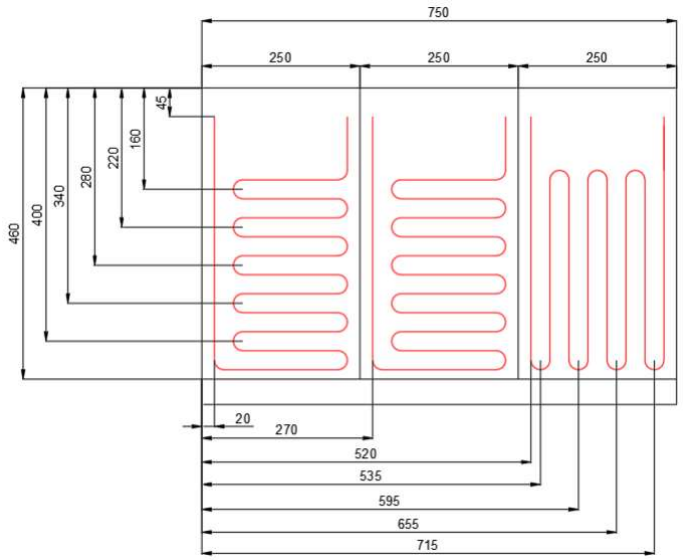

Figure 20: Geothermic arrnagement of coils with dimensions (Tofalo, Sperimentazione di muri energetici, 2019)

The coils, thanks to a system of valves, have the possibility of being selectively travelled in series or parallel by the fluid The flow is managed by a pump (GP2). The energy from the heat source is stored by it heating the brine a few degrees, from about –3 °C to about 0 °C.

B. Heated brine flows toward the evaporator of the heat pump and releases heat energy to the refrigerant and cools down a few degrees, then returns to the heat source to retrieve the heat again from the ground (figure 19).

2) Refrigerant circuit

C. An intermediate circuit is inside the pump and here R407C refrigerant with a very low boiling point absorbs the energy from brine and starts boiling until reach a saturated vapour phase in the evaporator
D. Refrigerant changes to gas and is routed into a compressor which is powered electrically. When the compressor compresses the gas, pressure and temperature increase considerably from approximately 5 °C to 100 °C
E. Compressed high temperature and pressure gas passed into the condenser where it releases its energy to end-user through a heat exchanger, whereupon the refrigerant is cooled and condenses to liquid phase again.
F. The fluid passes liquid form but it is still in high pressure, so we use here an expansion valve to decrease the pressure of the fluid and return its original point. And the cycle continues like that.

3) Heat medium circuit

G. In this circuit hot (or cold when we use the system as a cooler) water inside the Pacetti storage tank mod. 100l VTCFH with thermal flywheel function gains the energy from the refrigerant in a condenser heat exchanger and circulates to the final user. Here the water flow is managed by a pump (GP1)

H. The hot water heats the room by heat exchangers, in that case, it is Sabiana fan coil mod CRC24 (figure 15). This branch of the circuit can also be used for other purposes, such as transporting hot water to the sanitary facilities in the building, heating a swimming pool, etc. (NIBE, User manual)

The system is also equipped with a whole series of valves, which allow its control and the various safety regulatory functions for its protection and that of the people who could be in its vicinity. (Rondina, 2020)

Sensors

The sensors that characterize the Nibe geothermal plant mainly compost from temperature sensors. Those useful for this study will be listed below, which are graphically visible in figure 21a:

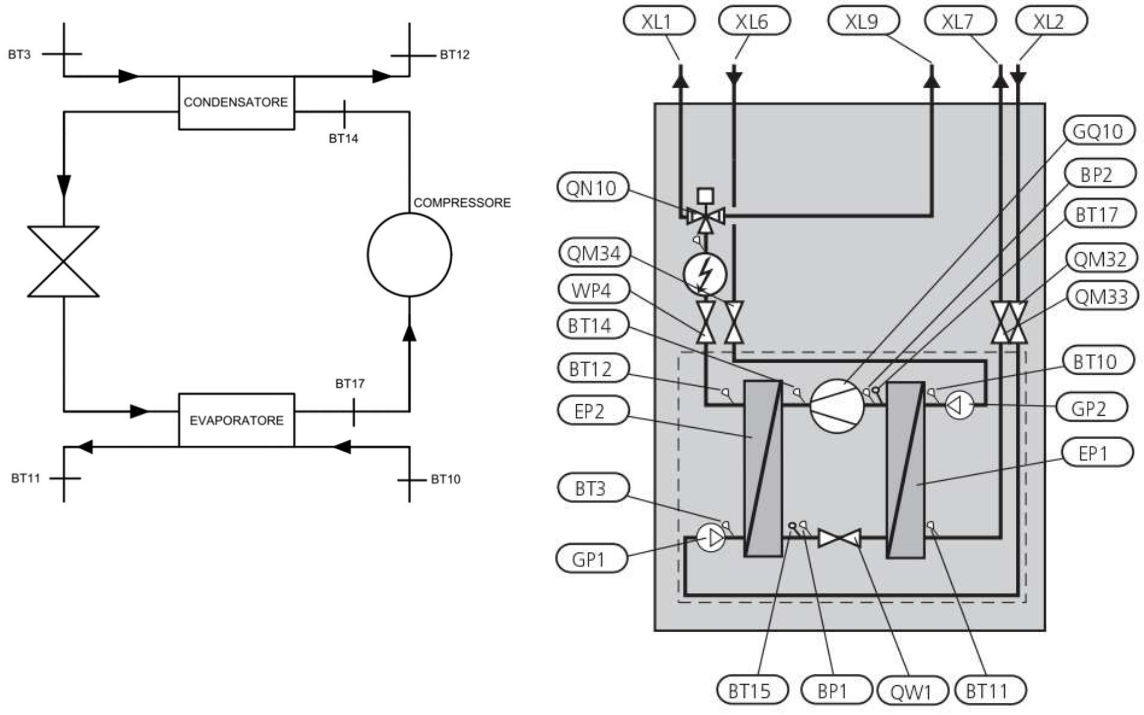

Figure 21 (a)Schematic drawing of the arrangement of the temperature sensors, and (b)other components of the pump

List of components

Pipe connections

XL 1	Connection, heating medium flow
XL 2	Connection, heating medium return
XL 6	Connection, brine in
XL 7	Connection, brine out
XL 9	Connection, hot water heater

Cooling components

EP 1	Evaporator
EP 2	Condenser
GQ 10	Compressor
QN 1	Expansion valve

HVAC components

GP 1	Circulation pump
GP 2	Brine pump
QM 32	Shut off valve, heating medium return
QM 33	Shut off valve, brine out
QM 34	Shut-off valve, brine in
QN 10	Shuttle valve, climate system/water heater
WP 4	Pipe connection, heating medium flow

	Name	Location	Function
BP1	High pressure pressostat	On the liquid line.	Protects the compressor against pressures that are too high.
BP2	Low pressure pressostat	On suction gas line.	Protects the compressor against pressures that are too low.
BT1*	Outside sensor	Outdoor, shaded location on north side of the house.	Set point values for heating and cooling demand calculation. Operating mode change.
BT2	Flow pipe	On flow line after immersion heater (EB1).	Calculation of DM. If BT25 is installed, only view.
BT3	Return pipe	On return line between circulation pump (GP1) and condenser (EP2).	Stopping the compressor at high temperature.
BT6*	Hot water, charging	On water heater lower section.	Stop and start of hot water charging. Also used for display if BT7 is not installed.
BT7*	Hot water, top	At water heater peak	View
BT10	Brine in	On incoming brine line before circulation pump (GP2).	View.
BT11	Brine out	On outgoing brine line after evaporator (EP1).	Stopping the compressor at low temperature.
BT12	Condenser flow line	On flow line between condenser (EP2) and immersion heater (EB1).	Stopping the compressor at high temperature.
BT14	Discharge	On hot gas line after compressor (GQ10).	Stopping the compressor at high temperature.
BT15	Fluid pipe	On the liquid line after the condenser (EP2).	View.
BT17	Suction gas	On suction gas line before the compressor (GQ10).	View.
BT25*	External flow line	Externally on the flow line to the heating system.	Calculation of DM. Actual value for additional heat mixing valve.
BT50*	Room sensor	In suitable indoor location.	Correction of the indoor temperature.

- outside temperature, BT1;
- return temperature of the heating fluid, BT3;
- the temperature of the return fluid from the probes, BT10;
- the temperature of the flowing fluid towards the probes, BT11;
- flow temperature from the condenser of the heating fluid, BT12;

- hot gas temperature, BT14;
- suction gas temperature, BT17.(figure 21a)

In the branch of the primary circuit, there is also a flow meter that allows a measurement of the flow rate of the water - propylene glycol solution, used in the extraction of heat from the ground. The machine can also measure the speed of the pumps serving the primary and secondary circuits. (Rondina, 2020)

Chapter 4 Case study

The main aim of this thesis is a comparison between the calculated values based on the ".txt" file data generated automatically by the electronic control unit of the Nibe F1155, and the results obtained from "Coolpack" software by inserting the same data. And also we will analyze and compare achieved results with documentation values which are given in technical data of NIBE F1155. By comparing the results, we can make sure whether there are problems at the operating level that preclude the use of this kind of heat pump in a residential environment. All the energy values, the exchanged powers, the flow rates, the efficiencies, any type of result, were calculated as instantaneous quantities for each of the approximately 4500 measurements with the compressor on (the measurements in all are approximately 20750). Subsequently, these quantities were averaged according to certain criteria, which vary from case to case, depending on what is to be highlighted in the given circumstance.

4.1 Collected data

The data used for the study derives almost entirely from the ".txt" file generated automatically by the electronic control unit of the Nibe F1155. The control unit measures a regular settable frequency (in this case every 30s) in which it stores the values measured by the sensors present inside the machine. We collect data from the control unit for 8 days (starting from 24/10/2019, ends 31/10/2019). We are analyzing the heat pump in the heating mode (winter season), that's why we used old data which was measured in 2019. The values useful for the study are the operating speeds of the GP1 and GP2 pumps, expressed as a percentage, and the temperatures described above. In the current state of the machine, there are no sensors that allow instant pressure measurement (it is necessary to purchase an accessory), but the manufacturer has stated that the high-pressure branch must work with a pressure between 16 bar and 30bar, while the low pressure one in a range of 7-11bar. In the thesis, we calculated the values for four different pressure ranges to understand the effect of pressure on the performance of heat pumps. These pressure ranges are *7-16 bar, 8-16* bar, *7-20 bar,* and *7.23 bars* which completely correspond to the allowed working pressure range of NIBE heat pumps. The last fundamental data is the one that derives from the measurement of the flow meters present on the branch of the primary circuit, that is, the one that leads to the underground probes. The flow rate value of *460=l/h*, (Tofalo, Sperimentazione di muri energetici, 2019) an average of the values measured by the flowmeters installed on the system, was exploited. By exporting the large data of the control unit to an excel file we can use all temperature values of the system to calculate desired values (COP, mass flow rate, heat exchanged powers between circuits, etc). In the data file, all temperatures are given $T(℃) * 10$ format in order to see variations clearly, because the system gathers sensors data every 30 s.

The Nibe F1155 geothermal heat pump operates very similarly to that of a boiler: it is not continuously active but turns on the compressor only when the system delivery temperature reaches a certain preset value. This value can be constant (as in the case of the test of this study) or characterized by a curve with which it is possible to more precisely adjust the supply of heat to the room to be heated according to the specific needs of each moment of the day. and external environmental conditions, optimizing the energy consumption of the machine. In the case of this test, the constant value of the delivery temperature to the home system set is equal to 45 °C and in fact, if one observes the trend of the BT12 in figure22. We can see from the figure that, the compressor starts working when

the temperature is lower than approx. 41℃, and turn off when it reaches about 51℃.

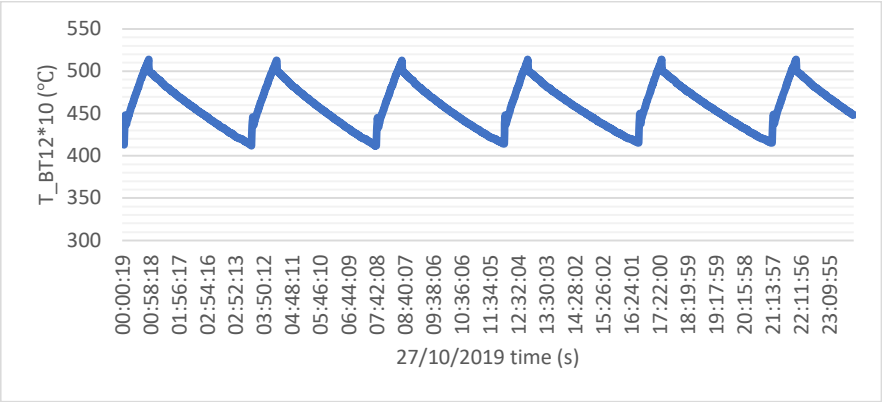

Figure 22: Explanatory graph of the trend of BT12 during the day of 27/10/2019

The control of the delivery temperature is carried out through the "Degree Minute" ($℃ \cdot min$)value that manages the switching on and off of the compressor. The values can be calculated using the following formula:

$$DM = \sum_{i=1}^{t_i} (T_a - T_s) \cdot t_i \qquad (1)$$

Here:

DM: degree minute [$℃ \cdot min$]

T_s: setpoint temperature of the heating curve (°C, 45 ° C in the case of this study),

$T_a$flow temperature in the current operating conditions (°C),

t_n: time passed (min) (Kaiser Ahmed 1, 2019).

When the cumulative value of DM reaches a certain number calculated by the machine control unit, the compressor will activate. In figure 23 the compressor works between highlighted line values (starts at -618 ends at 0) and stops outside of this range, and it repeats periodically.

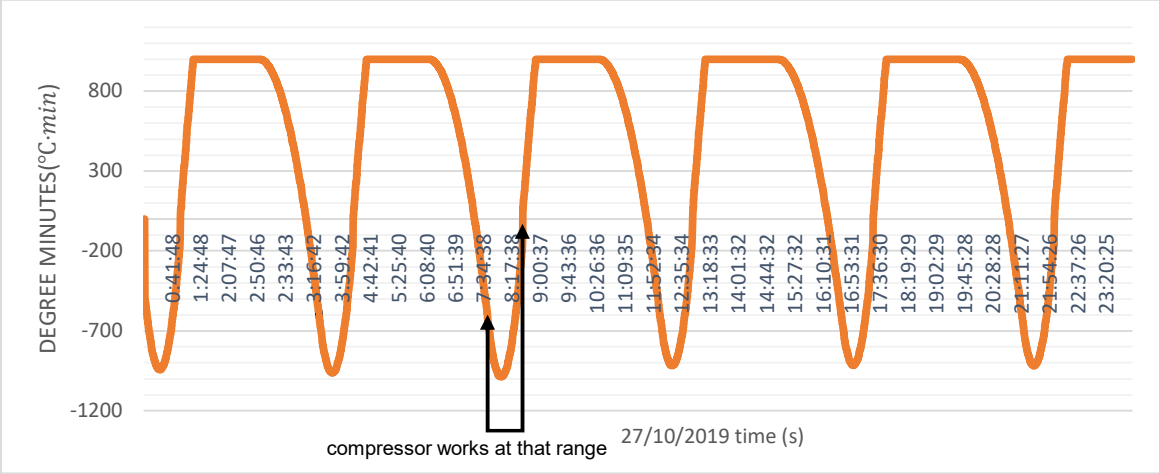

Figure 23: Degree minutes results of NIBE control for 1 day

To show an operating cycle, the period starting at 07:41:08 on 27/10/2019 with the compressor switching on, passes through 08:34:03, when the compressor switches off, is taken as a sample ends at 12:02:34 again on 27/10/2019, a moment before the compressor starts up again. The below figures show the temperature trends during this period of operation. As expected, the temperatures are different when the compressor is switched on, when the compressor switches off the temperatures upstream and downstream become the same, in the case of the exchangers (figure 24), while they decrease and get closer and closer in the case of the compressor(figure 25).

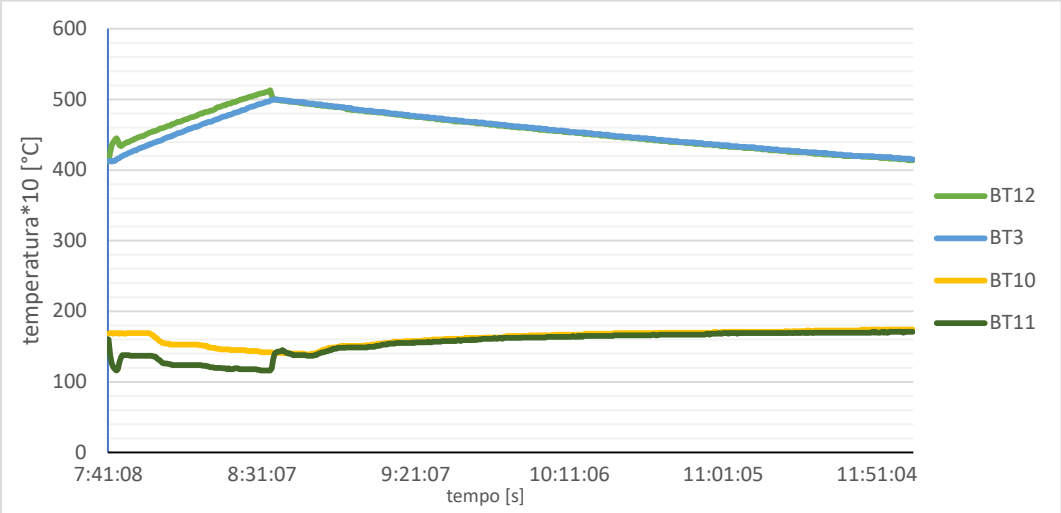

Figure 24: temperature trends of two heat exchangers.

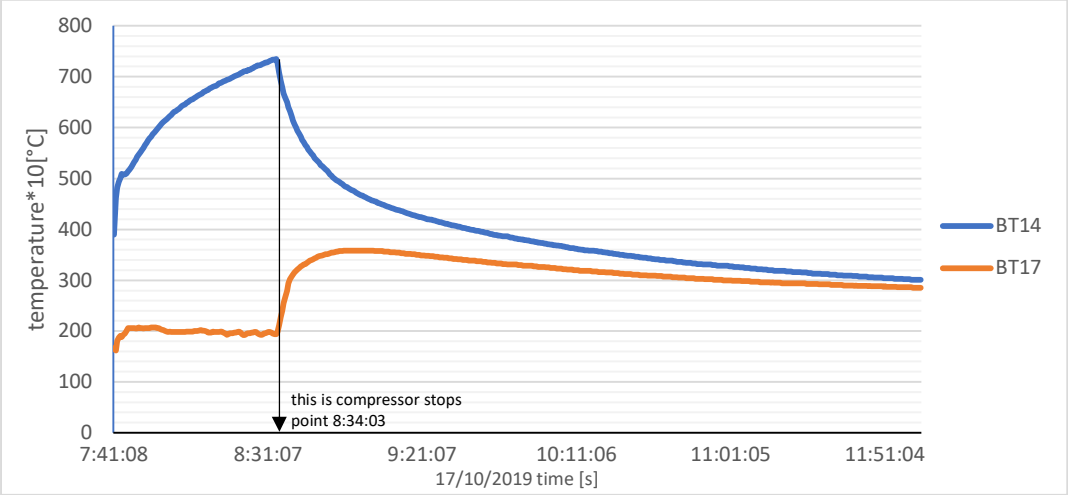

Figure 25: The temperature trends of compressor inlet (BT17) and outlet (BT14)

The important feature to consider is the fact that the compressor works in a superheated gas zone, this is because it must not have to deal with liquid particles of fluid during its operation. These particles would destabilize its performance and lead its components to premature wear. It is also interesting to note how the (log(p)-h) diagram of the R407C refrigerant is particular within the saturation curve: unlike that of other fluids, here the isobars within the curve are not also isotherms. Proceeding perfectly horizontally at a constant pressure it is noted that the temperature value on the lower limit curve will be lower than that intercepted on the upper limit curve. This implies that the change of state of the R407C refrigerant fluid from gas to liquid does not occur at a constant temperature (figure 26).

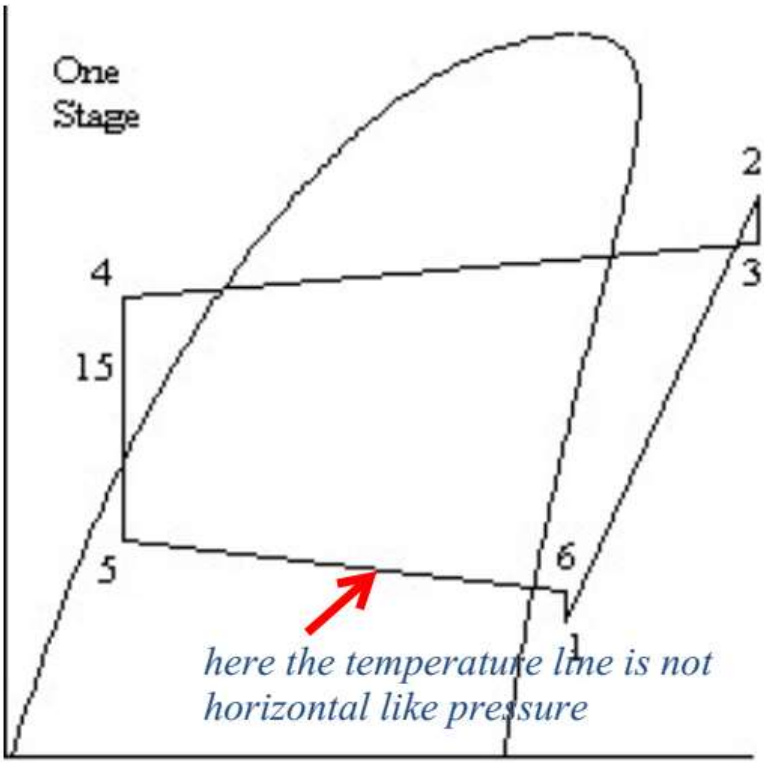

Figure 26: The Coolpack draw of refrigerant R407C for 7-16 bar

4.2 Assumptions

During the analysis, we need to do some hypotheses to complete the calculations clearly, because we have a lack of data in some parts of the calculation.

1) First of all concerning the pressures of the two branches: a constant pressure was considered, as it was not currently possible to have instant pressure measurements through the installed sensors. And we will discuss 4 different fixed pressure ranges to run Coolpack software as previously mentioned.
2) Regarding specific pressure heat constant (c_p) it is necessary to distinguish the three different circuits. In the primary circuit, it is seen that the variability of the c_p, for the 25% water-glycol mixture, is not so pronounced and therefore a constant value of 3.953 kJ/kgK. The same argument can be made on the secondary circuit, that of the flowing fluid. in which you are dealing with water with a c_p constant of 4.186 kJ/kgK. In the circuit inside the heat pump the c_p it is used to count the electrical power needed by the compressor. It works with very different temperatures and pressures during the day and

each of these operating points corresponds to a different specific heat. We will show how to find an average c_{pR407C} later.

3) The same argument can be made on the density of the secondary and primary fluids: their variability is very limited and for this reason, they are considered constant.

$$\rho_{glycol} = 1016.37\ \frac{kg}{m^3}, \qquad \rho_{water} = 1000\ \frac{kg}{m^3}$$

4) The flow rate of the primary circuit, like that of the secondary, is considered constant for the entire operating time, as it depends solely on the pump. In the machine settings, it is possible to choose how to make the pumps of the two circuits work and, in the specific case of this study, the pumps were set in manual mode, with constant speed fixed at 100%, regardless of the compressor on or off status.
5) Another fundamental assumption is that the refrigerant fluid does not undergo any under-cooling: (log(p)-h). It is necessary to make this hypothesis because there is no temperature data on this particular point of the cycle, as there is no sensor installed by the manufacturer in this specific position.
6) We use only data relating to the time moments in which the compressor is turned on is used for COP counts. In most parts of the measurement period, the pump was turned off. If the pump doesn't work, it is meaningless to calculate powers and performances.
7) The point at the capacitor outlet is considered on the lower boundary curve (of saturated liquid). When we build a Coolpack diagram, the cycle points will overlap slightly with the saturated liquid line, and it will cause some difficulties to take state values(figure 27).

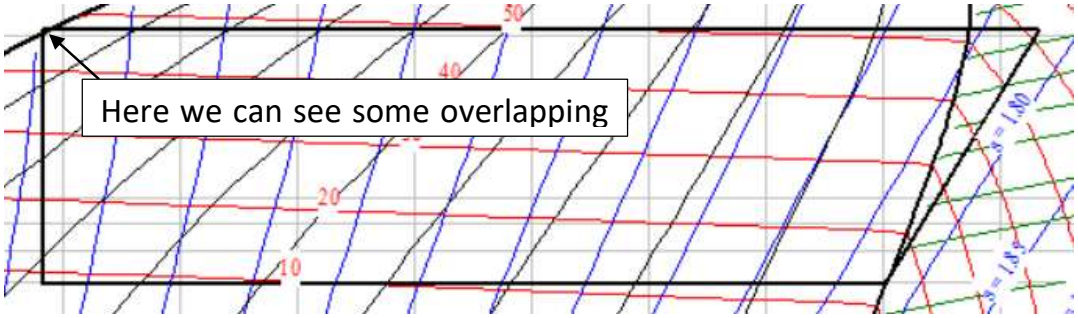

Figure 27: 7-16 bar cycle diagram of R407C

8) Enthalpies are obtained by linear interpolation: remarkable values are found manually through the tables (tools on Coolpack) as a function of pressure (set constant for hypothesis) and temperature (sensor), and excel function is applied to them.

9) Lastly, no losses of any kind are assumed, no pressure losses along the ducts, nor energy or heat losses in the exchangers, in the compressor, and the pipes.

4.3 COP of the system

The coefficient of performance (COP) of the system is a typical energy performance that is used when our heat pump works in heating mode and it is the ratio of useful heat provided by the system and the work done by the compressor of the heat pump

$$COP = \frac{\dot{Q}_H}{W_i} = \frac{q_{H,R407C}}{l_{i,R407C}} \; [-] \qquad (2)$$

$q_{H,R407C}$: specific heat exchanged in the condenser (hot side) $\left[\frac{kJ}{kg}\right]$

$l_{i,R407}$: is the work done per unit mass by the compressor and this is supply energy by external (electric energy) $\left[\frac{kJ}{kg}\right]$.

$\dot{Q}_H$: Heat exchanged in the condenser [kW]

W_i: Electric power used in the compressor [kW]

High COP means higher efficiency and lower power consumption thus lower operating costs. A contribution of irreversibility occurs at the lamination valve since it is not possible to bring all the fluid back to the initial pressure, while the most important internal irreversibility is due to the imperfect compression of the fluid. And these factors cause a reduction of COP approximately 50% of theoretical Carnot cycle efficiency due mostly to the temperature difference between the two sources.

$$COP_{Carnot} = \frac{T_H}{T_H - T_C} \qquad (3)$$

The energy efficiency of a heat engine increases if the temperatures of the two sources are close. That's why we are trying to use a hotter source during winter (ground) to reach a smaller temperature difference between the hot and cold sources.

In the summer case, if the thermodynamic cycle of the heat pump is reversed, we speak of active cooling, otherwise if the natural temperature difference between the geothermal probes and the ground is directly exploited, (without the use of the HP), the free cooling or natural cooling, for which special boundary conditions are necessary. During active cooling, the components of the HP do not change but its efficiency is quantified through the refrigeration Coefficient *energy efficiency ratio* (EER) or COP for cooling expressed as the ratio between the heat released from the internal environment and the work supplied:

$$EER = \frac{\dot{Q}_C}{W_i} \ [-] \tag{4}$$

$\dot{Q}_C$: heat power exchanged in the evaporator (cold side) $[kW]$.

EER is usually bigger than COP (Wikipedia, n.d.)

To calculate the COP of the heat pump we need to use specific quantities of energy because the mass flow rate of the refrigerant is not known. The heat losses can be neglected by approximating the compressor system as an adiabatic system, it can be considered that the compressor works only on the pressure and temperature of the fluid, keeping its speed unchanged, finally since the machine does not move during its operation, even the difference in gravitational energy can be considered null. Then:

$$l_{i,R407C} = c_{p,R407C}(T_{BT14} - T_{BT17}) \tag{5}$$

Here $c_{p,R40}$ is the specific thermal capacity of the refrigerant

It is important to check the temperatures of the BT17 sensor, because observing the available data and comparing them with the diagram (log(p) -h), some operating points at the compressor inlet (determined by temperature and pressure) are within the limit curve. This means that, at least in a part of the transformation, the compressor could find itself working with partially liquid rather than gaseous fluid, which would cause malfunctions or disservices. This fact depends on the hypothesis of constant pressure, mandatory due to lack of data, but which inevitably leads to critical issues. The actual operation of the compressor would have an initial transient, during which the pressure would gradually increase, allowing it to always work with totally gaseous fluid. That

said, the point on the curve is determined by the pressure of the low-pressure branch upper limit to which a temperature will correspond, T_{satLP}. At this point if $T_{satLP}<T_{BT17}$ the equation holds, then surely the compressor will work with totally gaseous fluid. All points that do not meet this condition have been discarded by the calculation of $l_{i,R407}$ and therefore of the COP. In the same way, it will also be necessary to check the temperature detected by the BT14 sensor: the same applies procedure followed on the low-pressure branch. The high pressure at the exit of the compressor, on the diagram (log (p) - h) you read the temperature (T_{satHP}) of the point at the intersection of the isobar and the upper saturation curve and, if $T_{satHP}<T_{BT14}$ then it means that the compressor also in this case works with a gaseous fluid. Again all points of operation detected by sensors, whose temperatures do not respect this inequality, must not be considered in the calculation of $l_{i,R407C}$ and the COP. The temperature controls described above have considerably reduced the range of variation of the pressure. If pressures higher than *23bar* in the high-pressure branch or higher an *8bar* for the low-pressure branch, the number of operating points to be excluded would be greater than 25% of the total, thus making the averages wrong. For this reason, the intervals considered in this analysis are *16-23bar* (for high pressure) and *7-8bar* (for low pressure).

Now we will show calculation steps of specific work done by the compressor for one day and one of the pressure ranges. As an example, we took the 27/10/2019 date and the 7-23bar pressure assumption. But at the ending of the analysis, we will give all days and all chosen pressure range results.

Firstly, we find some state values for chosen pressures by using a refrigerant calculator

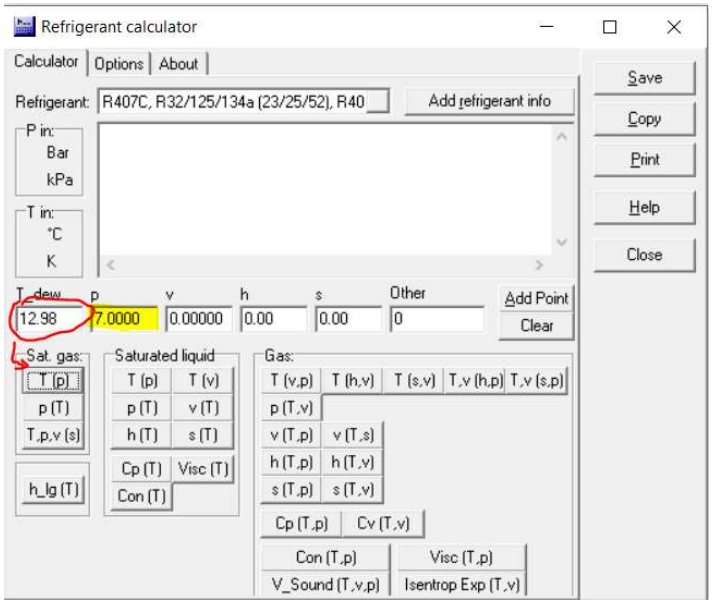

Figure 28: Refrigerant calculator. Input is pressure and output are saturated T and h

$p_L = 7bar$	$T_{sat\_gasLP} = 12.98℃$
$p_H = 23bar$	$h_{sat\_liq} = 286.44\ kJ/kgK$
	$T_{sat\_gasHP} = 56.34℃$
	$T_{sat\_liq} = 51.84\ ℃$

To find the c_{pR407} , we proceed by identifying the maximum and minimum temperature values of both the high-pressure part of the circuit (compressor outlet) and the low-pressure part (compressor inlet), considering the time of one day. By crossing these temperature values with those of the pressure, the c_p, corresponding to each working point was calculated by using the refrigerant calculator. Finally, an average was always made daily on identified values. The average specific heat will therefore be considered constant over the reference day. We can see in the below table how to find an average c_{pR407C}.

10/27/2019			
$c_{pR407C\_average}\ kJ/kgK$	1.059		
T_{minHP} °C	56.4	T_{minLP} °C	19.2
T_{maxHP} °C	73.5	T_{maxLP} °C	21.4
$c_{p\_maxHP}\ kJ/kgK$	1.273	$c_{p\_maxLP}\ kJ/kgK$	0.894
$c_{p\_minHP}\ kJ/kgK$	1.173	$c_{p\_minLP}\ kJ/kgK$	0.897

Now we can calculate instantaneous work done values of compressor for switching on conditions only. Here we will show average values of temperatures, and $l_{i,R407C}$ for 27/10/2019 date

27/10/2019	
T_{BT14_ave} °C	66.87
T_{BT17_ave} °C	20.31
$l_{i\_ave}\ kJ/kgK$	49.315

After calculating the specific work done by the compressor, we move on to consider the condenser, in which heat exchange takes place. In the condenser, heat exchange with the user (water in our case) is calculated through enthalpy differences between state points of condenser inlet and outlet.

$$q_{H,R407C} = h_{BT14} - h_{sat.liq} \quad (6)$$

h_{BT14}: Enthalpy at the compressor output$\left[\frac{kJ}{kgK}\right]$

$h_{sat,liq}$: Enthalpy of saturated liquid (high pressure)$\left[\frac{kJ}{kgK}\right]$

The end-of-transformation enthalpy ($h_{sat.liq}$), at the condenser outlet, it corresponds to that of the point at the intersection between the high-pressure isobar and the curve of lower saturation and is therefore constant, once a given pressure level is set. The enthalpy of the point at the input of the condenser instead is found through the diagram (log (p)-h), as a function of temperature and pressure. Not having available software that would allow a precise evaluation of this enthalpy for all the measurements made every30s from the Nibe control unit,

it was necessary to proceed differently. Operating points were randomly identified, the enthalpy of which was manually calculated through the diagram (log(p)-h). By exploiting a linear interpolation, all the enthalpy values of the other points were then obtained, in an automated manner through the spreadsheets. As an example here the random values of enthalpies corresponding to appropriate temperature points are chosen

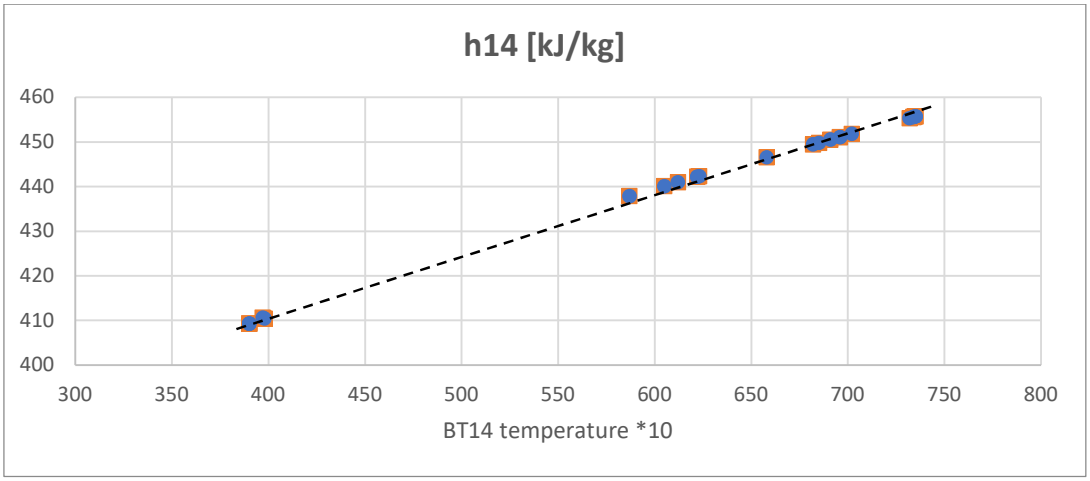

Figure 29: Linear interpolation of randomly calculated enthalpies for 27/10/2019

Finally, by carrying out sample checks, it was seen that the method followed led to having enthalpy values that differ very little from the real ones, therefore fully acceptable values for proceeding with the analysis.

Then we can calculate specific heat released by the condenser for each instantaneous value and then take an average

27/10/2019	
$q_{H,R407C\_ave}$ (kJ/kgK)	161.043

In conclusion, the COP was calculated as the ratio between heat exchanged and work for all those points where the compressor was on and for all those points that complied with the temperature controls described above. we have to skip some "no gas" values which cause misalignment of average values. Here we can show max and min COP was taken on 27th October and an average value for one day (figure 30).

27/10/2019	
COP_ave	3.29
COP_min	2.95
COP_max	3.93

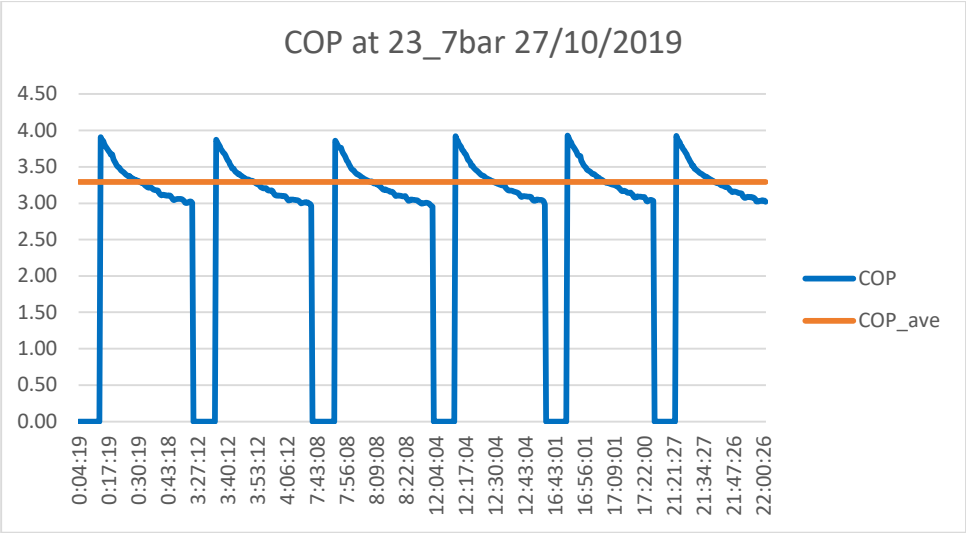

Figure 30: daily and average COP of the pump

4.4 Calculation of powers

The same statements made for the COP are also valid for the calculation of the powers: the operating points that involve the presence of liquid fluid inside the compressor are excluded and the calculations are made only for the operating points during which the compressor is on. . It would be useless to calculate the values of thermal power exchanged while the compressor is off because the refrigerant flow rate in that particular situation would be zero. In this part of the analysis, the flow rate value measured through the flowmeters comes into play. The only circuit whose flow rate is known is precisely the primary circuit, for this reason, the calculation of the powers must start from the evaporator, of which both the inlet and outlet temperatures on the primary circuit are known. The heat exchanged between brine and refrigerant circuits will be calculated by using this formula:

$$Q_C = \dot{m}_{glycol} \cdot c_{p,glycol} \cdot (T_{BT10} - T_{BT11}) \quad (7)$$

Here we have all data for the brine circuit. (Dusseldorf, 1991)

Density of glycol	ρ_{glycol}	*1026.3*	kg/m^3
Specific heat of glycol	$c_{p,glycol}$	*3.953*	*kJ/kg K*
Specific heat of water	$c_{p,water}$	*4.186*	*kJ/kg K*
Density of water	ρ_{glycol}	*1000*	kg/m^3
Volumetric flow rate	Q_{glycol}	*460*	*l/h*
Mass flow rate	$\dot{m}_{glycol}$	*0.1311*	*kg/s*

Without considering particular energy losses, it can be said that the heat released by the glycol, is the same that will be absorbed by the R407C refrigerant. Taking advantage of the power balance, it will also be possible to calculate the refrigerant flow rate in the circuit inside the heat pump by using the following calculation steps:

$$Q_H = Q_C + W_i \tag{8}$$

The heat released to the user is the sum of heat absorbed from the ground and supplied power to the compressor. If we write the equations of each power:

$$Q_H = \dot{m}_{R407C} \cdot q_{H,R407C} \tag{9}$$

$$W_i = \dot{m}_{R407C} \cdot l_{i,R407C} \tag{10}$$

$$Q_C = \dot{m}_{glycol} \cdot c_{p,glycol} \cdot (T_{BT10} - T_{BT11} \tag{11}$$

Now, by combining the above equations we can easily find the mass flow rate of the refrigerant fluid.

$$\dot{m}_{R407C} = \frac{\dot{m}_{glycol} \cdot c_{p,glycol} \cdot (T_{BT10} - T_{BT11})}{q_{H,R407C} -\cdot l_{i,R407C}} \tag{12}$$

By setting equality between the heat released by the refrigerant and that absorbed by the heating fluid, the water flow rate in the secondary circuit can also be easily found, which is constant (as expected given the constant operation of the GP1 pump). Here the temperatures of the secondary circuit can be measured with sensors.

$$Q_H = \dot{m}_{water} \cdot c_{p,water} \cdot (T_{BT12} - T_{BT3}) \quad (13)$$

$$\dot{m}_{water} = \frac{Q_H}{c_{p,water} \cdot (T_{BT12} - T_{BT3})} \quad (14)$$

27/10/2019			
The average mass flow rate of refrigerant	$\dot{m}_{R407C\_ave}$	*0.013*	*kg/s*
Average specific heat absorbed in evaporator	q_{C_ave}	*11.075*	*kJ/kg*

By summarizing all results we can get three main powers of the system are:

$$Q_C = \dot{m}_{glycol} \cdot c_{p,glycol} \cdot (T_{BT10} - T_{BT11}) \quad (15)$$

$$Q_H = \dot{m}_{R407C} \cdot q_{H,R407C} \quad (16)$$

$$W_i = \dot{m}_{R407C} \cdot l_{i,R407C} \quad (17)$$

27/10/2019			
Thermal power absorbed in evaporator (cold side)	$Q_{C,ave}$	*1.45*	*kW*
Thermal power released in condenser (hot side)	$Q_{H,ave}$	*2.09*	*kW*
Power supply to compressor	W_i	*0.64*	*kW*

In figure 31 we can see some drops in values of powers. These are because of “no gas” values since they will cause some to take wrong values.

Figure 31: Daily and average values of thermal and electrical powers 27/ 10/2019

4.5 Coolpack

Coolpack is software for refrigeration systems developed by the energy engineering department of the University of Denmark (CoolPack, 1995), in which there are different tools useful for the design or control of refrigerators, air conditioners, heat pumps, everything that works employing refrigerant fluid, for example, an R407C, as in the case of this study. The Coolpack tools that were used for this analysis are called "*Refrigerant Calculator*", which allows you to know the characteristic quantities of a point on the diagram (log (p)-h) having known, for example, temperature and pressure, "*Refrigeration Utilities*", with the function of drawing cycles on the diagrams (log (p) h), "*Heat transfer fluids calculator*", with which the characteristics of the primary circuit fluid can be calculated such as density, heat exchange coefficients or others, "*Cycle analysis*", with which it was possible to analyze the energy quantities and efficiencies of a thermodynamic cycle. The Refrigerant Calculator was fundamental in the analysis of the COPs to identify the remarkable enthalpies, on which to build the linear interpolation and c_p for the transformation that occurs in the compressor and the values of the points placed on the limit curves. The Heat

transfer fluids calculator was used to verify that the characteristics of the primary fluid (water propylene glycol) remained constant in the range of use. Through the Cycle analysis, it was possible to compare the calorific powers and the electric powers calculated on Excel, with the quantities calculated by the program itself. The tool offers various possibilities for entering data, and it has been chosen to enter the following quantities in the software: mass flow rate of the refrigerant fluid, electrical power required by the compressor, inlet, and outlet temperature from the compressor. The program calculates the powers exchanged in the condenser and evaporator, the COP, and various efficiencies.

Here we will show how to build a heat pump model in Coolpack software for 27/10/2019 day and 7-23 bar pressure range. But we have built these diagrams for all days and all pressures in excel, and we will show all results in the next subchapter.

4.5.1 Heat transfer fluids calculator

As mentioned above, it is used for finding the characteristics of brine fluid, in our case, it is a water-glycol mixture. We select propylene glycol from the fluid types section and we set the percentage of concentration 25% and we enter an approx. working temperature (20℃) we can take desired values for example the density, conductivity, specific heat capacity, and possible working temperature range(figure 32).

$$\rho_{glycol} = 1023.44\ kg/m^3$$

$$c_{p\_glycol} = 3.917\ kJ/kgK$$

$$\lambda_{glyccol} = 0.467\ W/mK$$

These results differ a little than we used during calculations because previous results were taken as average values corresponding to different temperatures. But this calculator is easy to use and there are enormous opportunities.

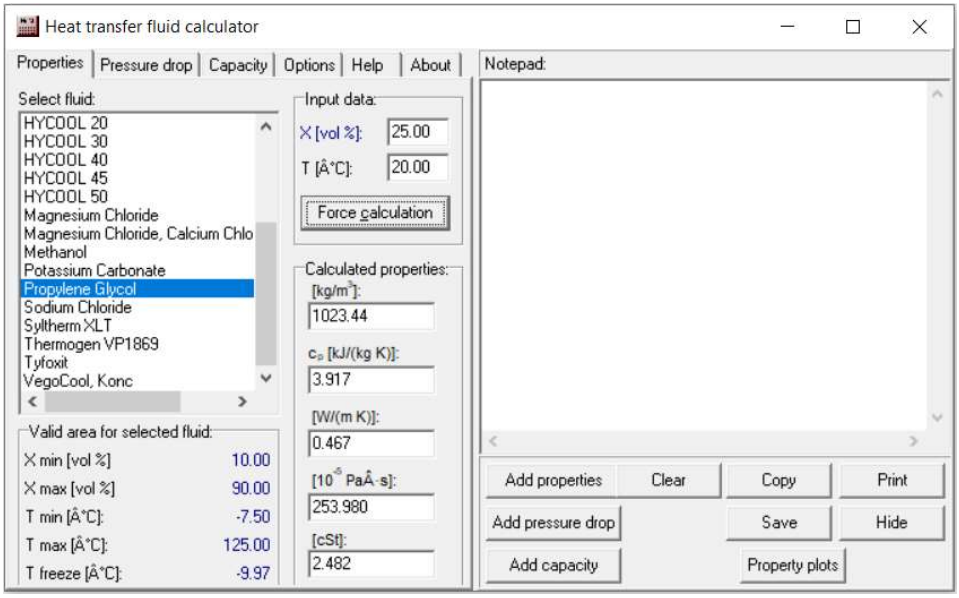

Figure 32: Heat transfer fluids calculator of Coolpack software

4.5.2 Refrigerant utilities

`This section helps us to draw the cycle in (log(p)-h) (Mollier) diagram.

When we enter the values we use a refrigerant calculator to find state points of the cycle for a given pressure range.

$p_L = 7bar$	$T_{sat\_gasLP} = 12.98℃$
$p_H = 23bar$	$T_{sat\_gasHP} = 56.34℃$
	$T_{sat\_liq} = 51.84\ ℃$

When we launch this section we choose a refrigerant type (R407C), select one stage cycle, enter evaporating and condensing temperatures which were found by the refrigerant calculator, and set the isentropic efficiency to 07 as the worst condition (figure 33).

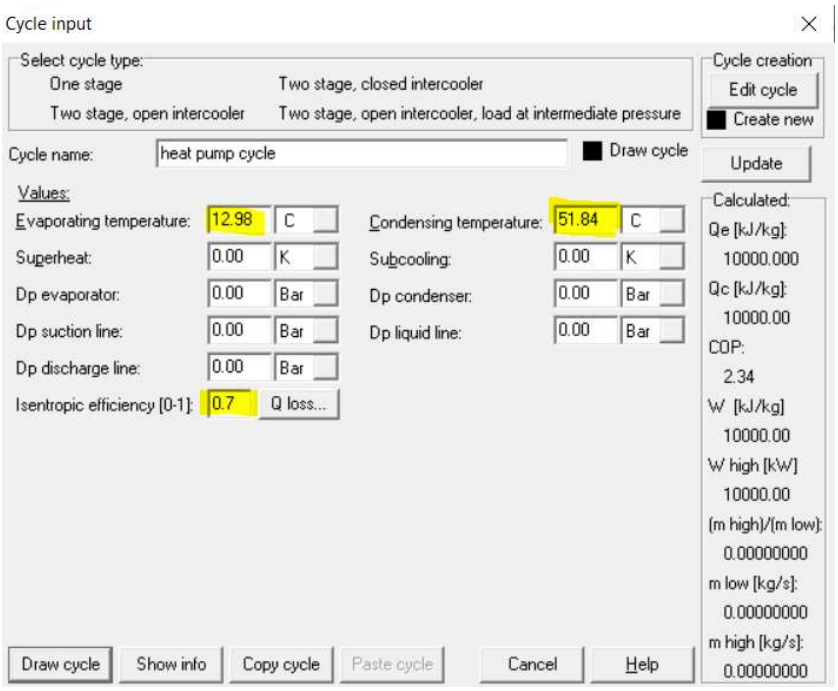

Figure 33: Data input window of refrigerant utility.

And the program will draw the cycle for 7-23 bar pressure in the log(p)-h diagram, as shown in figure 34

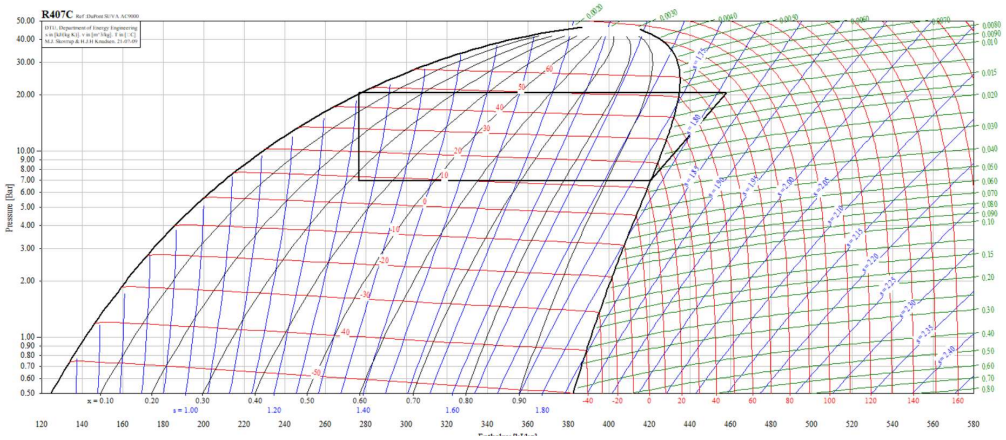

Figure 34: Cycle of the heat pump in Mollier diagram for R407C

Also, we can take coordinate points and the actual path of the cycle by printing the results in pdf file. This helps us to create a document about calculations in software(figure 35).

Refrigerant: R407C
Values at points 1-6,15 for the selected one stage cycle

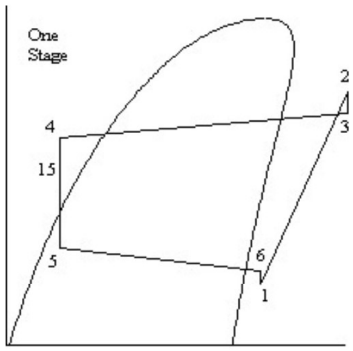

Point	T	P	v	h	s
1	12.801	6.959	0.034517	420.415	1.7798
2	72.034	20.510	0.012581	457.878	1.8128
3	72.034	20.510	0.012581	457.878	1.8128
4	46.845	20.510	N/A	276.725	N/A
5	N/A	6.959	N/A	276.725	N/A
6	12.801	6.959	0.034517	420.415	1.7798
15	N/A	20.510	N/A	276.725	N/A

Figure 35: coordinate values of the cycle, and actual cycle path.

4.5.3 Cycle analysis

One of the main parts of our study is to calculate the COP of the heat pump through the Coolpack software, and this can be done in the cycle analysis section. To calculate all desired quantities we have to input some state values which were taken from the refrigerant calculator and calculated by using control unit data. We build the cycle analysis for 4 pressure ranges and all 8 days, and we compare the results with the average values of each day. Also here we show only for one day (27/10/2019) and one pressure range (7-23bar) as an example.

We have already the state results for temperatures and mass flow rate of refrigerant for each day corresponding pressures, and also we enter the power supplied to compressor and average daily upstream and downstream temperatures of the compressor which were calculated in the COP part of the analysis. Here is the necessary input data for cycle analysis in the cycle specifications window and software calculates automatically COP and thermal powers in evaporator and condenser.

27/10/2019 7-23bar	
T_{sat_gasLP}	12.98℃
T_{sat_gasHP}	56.34℃
T_{sat_liq}	51.84 ℃
W_i	0.64 kW
$\dot{m}_{R407C\_ave}$	*0.013 kg/s*
T_{BT14_ave}	66.87 ℃
T_{BT17_ave}	20.31 ℃

Figure 36: Input data section of cycle analysis.

And by calculating system builds a closed cycle of the system and shows all calculated values on it.

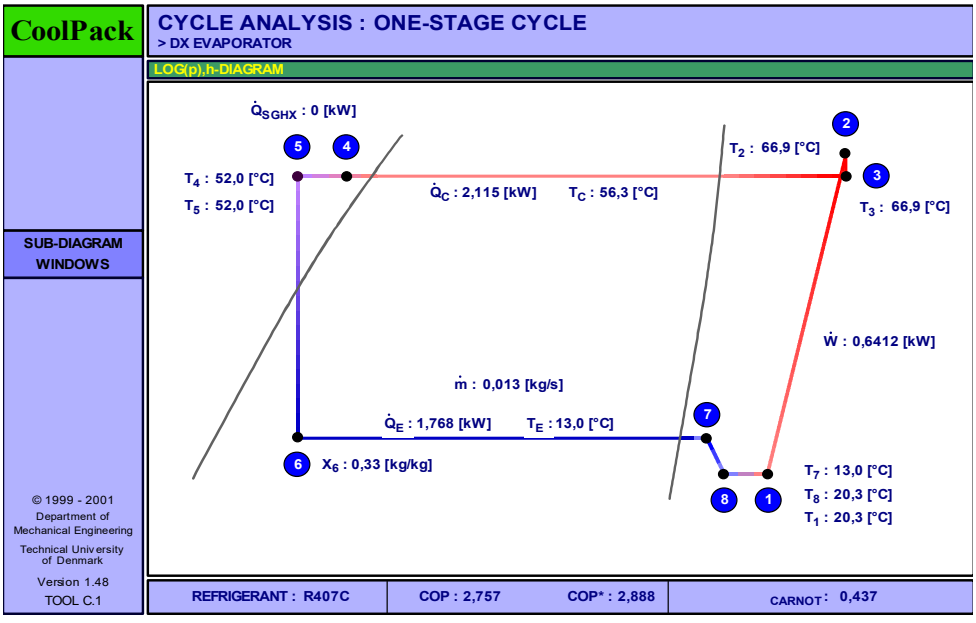

Figure 37: The cycle analysis diagram for 7-16bar and 27/10/2019

Achieved results are:

27/10/2019 7-23bar		
	Calculated in excel	Calculated in Coolpack
$Q_{C,ave}\ kW$	*1.45*	1.768
$Q_{H,ave}\ kW$	*2.09*	2.115
COP	3.290	3.295

Attention: as we can see in the Coolpack display, the COP value is calculated, but that COP value was taken from the ratio of thermal power absorbed by the condenser and power supply on the compressor. Because all refrigeration cycles were focused on cooling the environment and their COPs are given according to these criteria. However, our goal is to heat the user by taking energy from the ground and useful power is released power in the condenser. In our case, we have to calculate COP of Coolpack results manually by using calculated powers in Coolpack.

$$COP = \frac{Q_{H,coolp}}{W_i} \tag{18}$$

The results of Coolpack are slightly different from calculated ones. Because Coolpack takes into account some energy losses and isentropic efficiencies automatically which we considered as no losses and without efficiency drops.

4.6 Summarizing the results

4.6.1 Comparison of COP values

After calculations, we achieve numerous results from excel and Coolpack. First of all, we pay attention to the COP of the heat pump in the analyzed periods. And can see that, COP of the system strongly depends on the external environment temperature, upstream and downstream pressures of the heat pump, and also heat losses during the cycle. In addition, we have to say that all the COP results are lower than the design value COP_d which is given in the installer manual document. For example, for 12℃ external temperature COP_d=4.86 (NIBE, NIBE F1155 Installer manual) They must be lower as the theoretical efficiency is generally always greater than the real one, calculated on experimental data. All the more reason, the external temperatures on which this analysis is based are even higher than the temperature at which the calculation was made to determine the COP_d. This means that if this study had been carried out on external temperatures around 12 ° C, then surely the calculated COP would have been lower than the COP_d,

10/2019	T_ave ℃	7-16bar		8-16bar		7-20bar		7-23bar	
days	external	COP_ave	COP_colp	COP_ave	COP_colp	COP_ave	COP_colp	COP_ave	COP_colp
24	16.2	4.85	4.584	4.66	4.470	3.82	3.757	3.16	3.171
25	16.3	4.70	4.585	4.68	4.565	3.94	3.888	3.29	3.296
26	16.6	4.73	4.613	4.68	4.569	3.95	3.891	3.29	3.295
27	16.7	5.02	4.617	4.97	4.567	3.95	3.896	3.29	3.299
28	17.2	4.77	4.652	4.72	4.307	3.98	3.927	3.32	3.325
29	17.3	4.71	4.587	4.68	4.558	3.93	3.873	3.29	3.295
30	16.9	4.61	4.486	4.57	4.450	3.83	3.775	3.23	3.232
31	13.8	4.41	4.302	4.35	4.250	3.66	3.610	3.10	3.109

Table 2: Calculated average COP and COP of Coolpack fir each day and each pressure set

If the external temperature is high then also COP of the system will be a higher value. It can be noticed very quickly is how the lowest average daily COP was obtained on the last day of operation (31/10/2019). By looking at the below table, we understand how this is determined by the fact that the outside temperature was significantly lower than in the previous days. 13.8 ℃.

The next important factor is that chosen pressure ranges are straightly dependent on the COP and if the lower and higher pressures are close then COP

of the system will be greater. From the table, it can be seen that the highest COP values correspond to the 7-16bar pressure set while the lowest ones were taken in the 7-23 bar pressure setting calculations. Also, we can easily understand from figure 38 how COP depends on the pressure range. The COP trends for 7-16 bar and 8-16 bar conditions are very close because their pressure ranges close to each other. Some zero drops in the graph are because of "no gas" conditions

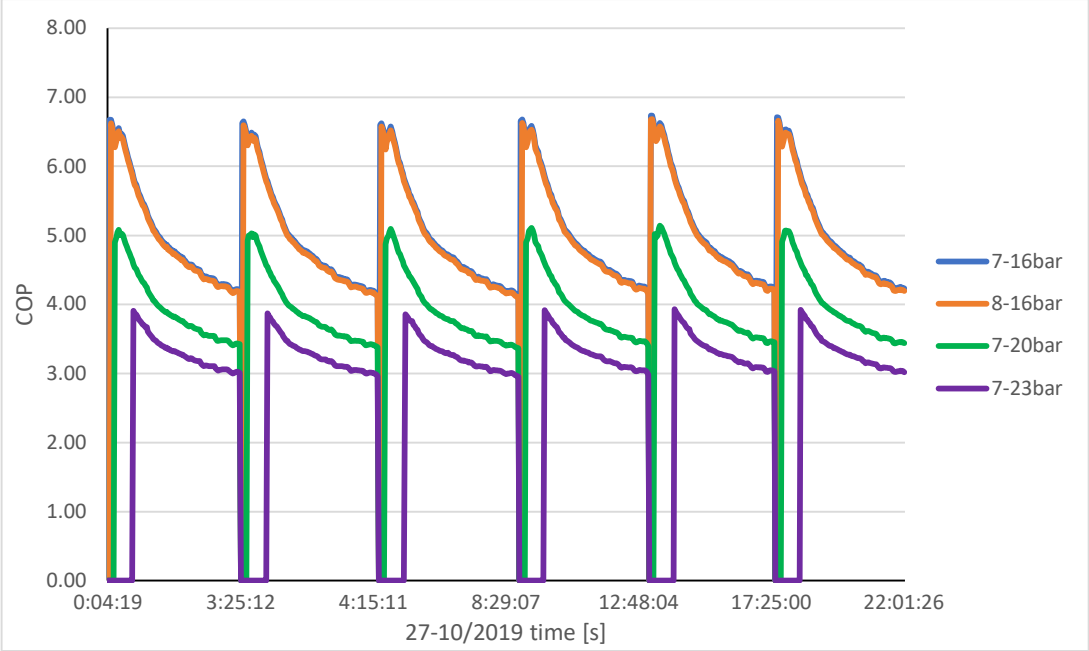

Figure 38: The daily COPvalues of each pressure settings for the 27/10/2019 day

Finally, the main important comparison is between the calculated results on excel and Coolpack software. And almost all COPs taken from Coolpack were lower than the average results calculated on excel. But in the last pressure range, the COP of Coolpack is slightly greater than the calculated one. This is due to pressure range because at high-pressure settings COP of the system drops dramatically. We can explain this difference with the consideration of losses and assumptions. In the beginning, we considered several hypotheses to calculate on excel, but Coolpack never ignore some irreversibilities during the cycle analysis and they affect the results surely. In reality, we cannot avoid some losses in the condenser, compressor, and evaporator. But differences are not enormous and this can be a factor to consider that our heat pump is working regularly. Here we will show percentage differences of measured and Coolpack COP results.

Table 3: percentage difference of COP between calculated and Coolpack results

	7-16bar		8-16bar		7-20bar		7-23bar	
10/2019 days	26	27	28	30	27	31	27	29
COP_ave	4.73	5.02	4.72	4.57	3.95	3.66	3.29	3.29
COP_colp	4.613	4.617	4.307	4.45	3.896	3.61	3.299	3.295
Diff in %	2.54	8.73	9.59	2.70	1.39	1.39	-0.27	-0.15

We can see from the table that lower pressure ranges cause greater COP difference between the calculated and Coolpack data. In figure 39 and figure 40 we show the trendlines of calculated and Coolpack COP values for randomly selected pressures and days.

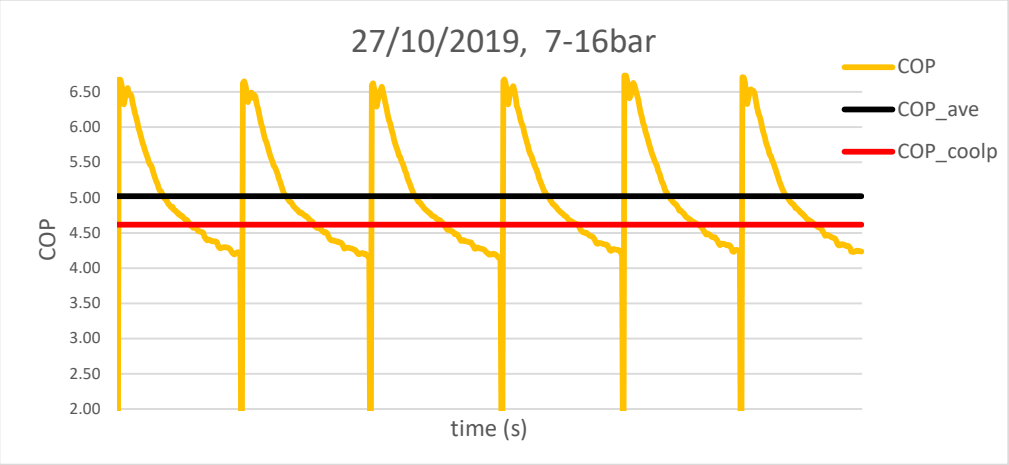

Figure 39:The daily, average, and Coolpack COP for 27/10/2019 at 7-16bar

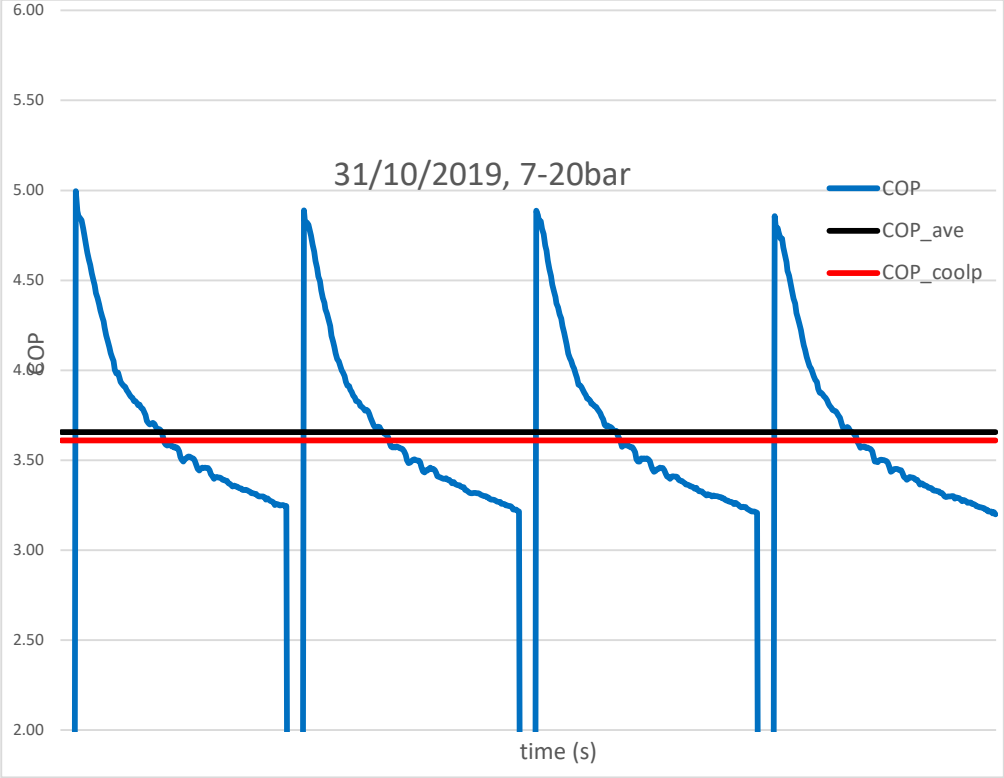

Figure 40: The daily, average, and Coolpack COP 31/10/2019 at 7-20bar

4.6.2 Comparison of thermal powers results

For thermal power exchanged in condenser we can conclude that higher pressure difference provides more energy to heat the user because in the compression process the refrigerant fluid increases its pressure and temperature and as a result, the fluid will give more thermal power. The thermal and electrical powers and also COP for the 24/10/2019 date are relatively higher than other days, while in other results days' results are not different strongly. We can explain this condition by looking at the achieved data from the NIBE control system. And on this day the heat pump was active only 4 times in 24 hours, but on other days the heat pump was switched on 7-8 times. When we calculate average values for each day the results for 24th October were different. As mentioned before, the compressor wasn't active always, and its working time was from 20 min to one hour on average. Then it stopped 3-4 hours and so on.

Table 4: the average and Coolpack values of thermal power in kW for all days and pressure sets.

10/2019	7-16bar		8-16bar		7-20bar		7-23bar	
	$\dot{Q}_{H,ave}$	$\dot{Q}_{H,coolp}$	$\dot{Q}_{H,ave}$	$\dot{Q}_{H,coolp}$	$\dot{Q}_{H,ave}$	$\dot{Q}_{H,coolp}$	$\dot{Q}_{H,ave}$	$\dot{Q}_{H,coolp}$
24	3.177	3.128	2.909	2.874	3.394	3.414	4.151	3.618
25	1.949	1.947	1.952	1.950	2.020	2.03	2.089	2.111
26	1.949	1.942	1.949	1.947	2.016	2.026	2.086	2.107
27	1.944	1.814	1.928	1.816	2.029	2.038	2.094	2.115
28	1.962	1.959	1.966	1.834	2.037	2.047	2.096	2.118
29	1.961	1.959	1.966	1.964	2.027	2.035	2.105	2.125
30	1.914	1.911	1.923	1.920	1.970	1.978	2.074	2.094
31	1.922	1.920	1.837	1.834	1.902	1.908	2.009	2.028

We can show in figure 41 the released power trends for different pressure ranges for the randomly selected day

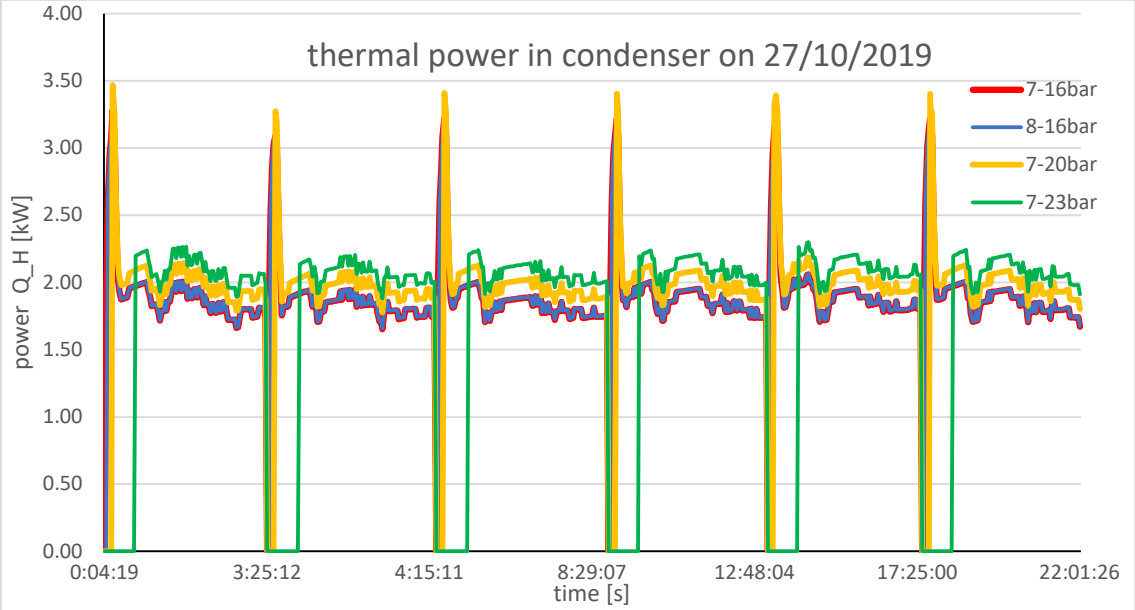

Figure 41: daily thermal power exchanged in condenser on 27/10/2019

For electrical power supplied on compressor we can give information for different days and different pressures, but not for calculated and Coolpack values. Because we used the average values of power as an input value for Coolpack.

Table 5: Average electrical power consumed by the compressor for all days and pressures

W_i (kW)				
10/2019	7-16bar	8-16bar	7-20bar	7-23bar
24	0.682	0.643	0.909	1.141
25	0.425	0.427	0.522	0.641
26	0.421	0.426	0.521	0.640
27	0.393	0.398	0.523	0.641
28	0.421	0.426	0.521	0.637
29	0.427	0.431	0.525	0.645
30	0.426	0.432	0.524	0.648
31	0.446	0.432	0.529	0.652

The highest power (highlighted in the yellow cell) was consumed on the last day because the external temperature dropped dramatically than other days and in the case of a high-pressure set (7-23bar). The results of the first day (light green cells) are different than others because of not enough active periods of the pump. So we don't pay attention strongly on this day. On the contrary, if we observe the power trends in figure 42, we can see how they grow as the pressure level increases, clearly denoting a greater energy demand by the compressor because if we want more compression (higher pressure) we must give more energy.

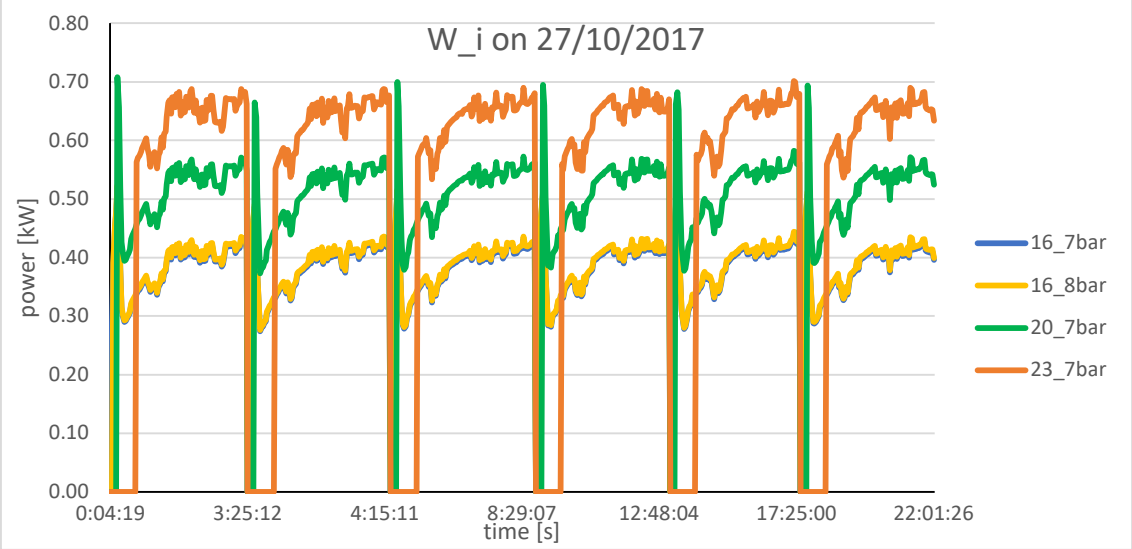

Figure 42: The daily power supply trends for different pressure ranges on 27/10/2019

The above figures show COP, Q_H, and W_i trends with the foresight that the moments in which the compressor is off are not represented on the abscissa axis, so everything is condensed for a better graphic rendering. In any case, the average operating COP calculated for each degree of pressure for the entire duration to which these data refer is 4.12, while the average value of COP_coolpack is 4.025 and these values respect what was previously stated regarding the COP_d.

Table 6:percentage increase of thermal and electrical power in different pressures for 28/10/2019

	Pressure levels ratio 8-16bar/7-16bar	Pressure levels ratio 7-20bar/7-16bar	Pressure levels ratio 23-7bar/20-7bar
% increase of average $\dot{Q}_H$	0.22	3.84	2.92
%increase of average W_i	1.12	23.78	22.22

Table 6 shows the average percentage increases in power linked to different operating pressure levels, relating to the day of 28/10/2019. It should be noted how an increase on the high-pressure line is more functional than an increase in pressure relative to the low-pressure branch, to obtain a higher output heat. An increase of one bar on the low-pressure line only increases by 0.22% the heat exchanged with the secondary fluid. It can be stated that on average with an increase in pressure of 1 bar on the high-pressure branch, the $\dot{Q}_H$ increases by approx. 1%; at the same time W_i, to allow a 1bar rise on the high-pressure line, it must however increase by about 8% on average. With this, we understand how actually in energy terms it is expensive to generate even a simple bar, but on the other hand, if the working conditions require a certain level of pressure, this will be an inevitable consequence.

Another fact that certainly needs to be mentioned, are the peaks that characterize the trend of $\dot{Q}_H$ and W_i at the beginning of the working cycle of the compressor, which occurs with the pressure levels 16-7 bar, 16-8 bar, and 20-7 bar (figure 43).

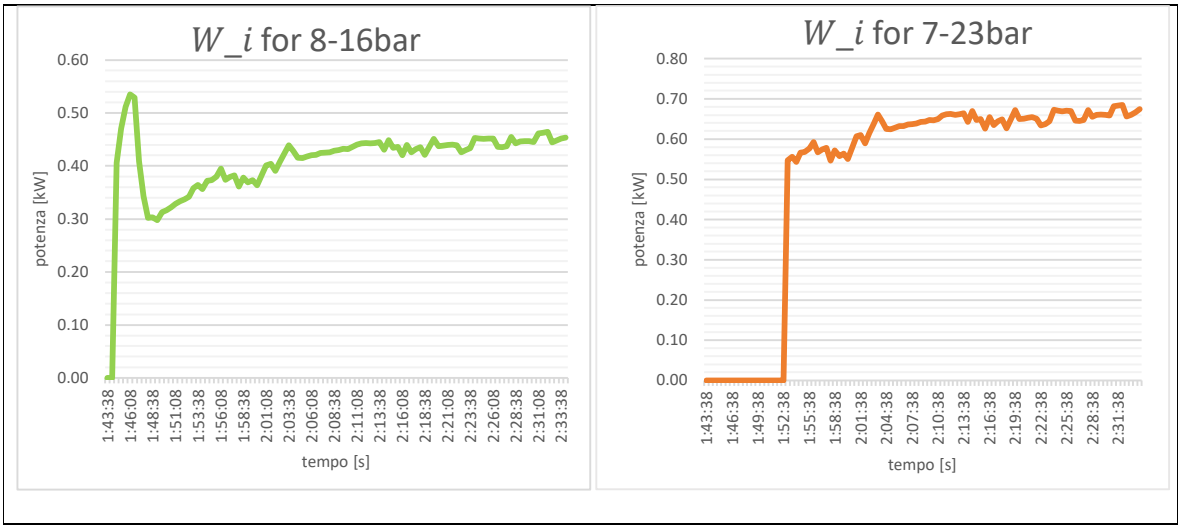

Figure 43: Trends of W_i in a cycle that starts from the start of the compressor until it stops, on 26/10/2019 from 01:43:38 to 02:34:08. On the left with the pressure level 16 8bar, on the right 23 7bar.

We know that the compressor job is not continuous and is therefore affected by not being able to work continuously in a steady state. These peaks occur due to the constant pressure hypothesis that was necessary due to the lack of instantaneous data on it: when the compressor is switched on, it is characterized by a transient phase, which could not be taken into account exactly for this reason. Not being able to properly deal with this aspect, anomalies were created in the calculations visible precisely in the form of power peaks at ignition. These power surges, on the other hand, did not occur for the pressure level 23-7 bar, which is justifiable because in this case, as previously stated, more data had to be discarded due to temperature controls. These controls led to the exclusion of those values close to the relative instants of time when the compressor is switched on (in figure 43 on the right, the first 10 minutes). Therefore not being part of the calculation, because excluded, they did not lead to the creation of any type of peak on the graph.

Conclusion

Generally, people think of ground source heat pump systems as a new and unknown technology, but it is not. Simply, a geothermal system has no visual impact, so it is impossible to understand if a building is powered by this type of system.

The results obtained from this analysis led to the conclusion that a geothermal heat pump can be safely used even in a residential environment because its operation does not present any type of acute abnormality. Furthermore, the use of a machine of this type would certainly bring benefits in those environments where there is the need for relocation of harmful emissions. However, its high installation cost would be recovered over time thanks to very low consumption, especially if combined with low-emission energy production methods (such as wind installations or solar panels). These high costs mean that they are still quite niche installations, however part of a rapidly expanding market, but progress and research will certainly help make them a more democratic product.

We have to comment also the cost-efficient factors to install these systems. First of all, cost strongly depends on the new or old building type. If the building was already built we will spend a relatively high amount of capital to install the brine pipes around the building. But if we install the geothermal circuit parallel with the building construction we will save the excavation spending, because we can install the underground pipes with other wiring systems (electricity, water, and drainage systems). For example, the total installation cost of our NIBE GHP system was around 30,000 euros (more expensive than usual), and the main factor is that the building was already built. My suggestion is that if we want to construct a new building we have to take into account the geothermal system installation because in the coming years this energy type will be the best choice for the HVAC system of buildings

Moving on to the more analytical level of the study, it should be noted that some hypotheses, such as those of pressure constancy, have proved to be very binding, so if you want to further investigate this analysis, pressure sensors should be mounted on the heat pump circuit. Having instantaneous data, accuracy will certainly be better, especially if a program is also used that allows you to accurately calculate the enthalpy values at the compressor output (remember that in this study they were identified by linear interpolation). With all these precautions, even more so, it would also be possible to take into account the transients present when the compressor is switched on, obtaining a complete

survey. Also, we can increase the COP of the system by installing a brine circuit more deeply and a better conductivity soil place. Because in the center the brine circuit pipes were installed after the completion of the building and there wasn't enough available place to mount them.

Another suggestion is that we can increase the performance of the heating by using the solar heating system which was installed on the roof of the building and it helps us to warm up the ground where is the energy source of our brine circuit and we use this system in winter seasons (after December). And as a result, in extremely cold weather periods the ground can heat the brine circuit to desired temperatures. we will save some energy consumption of the compressor by keeping the same COP.

Acknowledgment

I would like to express my deepest appreciation to my advisor, Mr. Davide Papurello, whose sincerity and encouragement I will never forget. He is the true definition of a leader and the ultimate role model. This thesis would not have been possible without his advice from the earliest stage of research enabled me to develop an understanding of the subject. I am grateful for the incredible experiences he has organized for me and for providing me opportunities to grow professionally. It is an honor to learn from Mr. Davide

I am grateful to my parents whose constant love and support keep me motivated and confident. My achievements and my success are due to the fact that they believed in me. A big thank you to my brothers and sisters, who keep me grounded, remind me of what is important in life, and always support me in my adventures. Also, I owe my deepest thanks to my love. I am eternally grateful for the unconditional love and support throughout the thesis process and every day. Finally, I have to say my gratuities to my friends, to my professors, and to the Polito University administration.

Bibliography

Aniko Toth, E. B. (2017,). *"Flow and heat transfer in geothermal systems".*

Bahtiyar Dursun, C. G. (2011). The role of geothermal energy in sustainable. *ENERGY EXPLORATION*, 207-209. Retrieved from https://journals.sagepub.com/doi/pdf/10.1260/0144-5987.30.2.207

CoolPack. (1995). Retrieved from https://www.ipu.dk/products/coolpack/

Course_GT. (n.d.). *SHALLOW GEOTHERMAL SYSTEMS.* Retrieved from https://geothermalcommunities.eu/assets/presentation/5.Course_GT.pdf

Dusseldorf. (1991). *properties of water-glycol*. Retrieved from https://detector-cooling.web.cern.ch/data/Table%208-3-1.htm

GEONOVIS energia geotermica. (2019). Retrieved from geonovis.com: https://www.geonovis.com/geotermia/prodotti/nibe-f1155/

Geothermal energy. (n.d.). Retrieved from the green network: https://greennetwork.it/en/renewable-energy-sources/renewable-sources/geothermal-energy/

IOP Institute of physics. (n.d.). *Ground source heat pump*. Retrieved from https://www.iop.org/explore-physics/sustainable-building-design/ground-source-heat-pump#gref

J. Lund1, B. S. (2004). GEOTHERMAL (GROUND-SOURCE) HEAT PUMPS. *ResearchGate* , 1-2.

Kaiser Ahmed 1, *. J. (2019). Modeling an Alternate Operational Ground Source Heat Pump for Combined Space Heating and Domestic Hot Water Power Sizing. *https://www.mdpi.com/*, 9.

M.H. Dickson, M. F. (1990). *Geothermal energy and its utilization*. Retrieved from https://www-sciencedirect-com.ezproxy.biblio.polito.it/science/article/pii/S0375650500000560#BIB9

Manzella, A. (n.d.). Geothermal energy. *Institute of Geosciences and Earth Resources*.

Meho Saša Kovačević, M. B. (2013). *Possibilities of underground engineering for the use of shallow geothermal energy.* Retrieved from https://www.researchgate.net/publication/278392855_Possibilities_of_underground_engineering_in_the_use_of_shallow_geothermal_energy

NIBE. (n.d.). User manual. 9-10.

NIBE. (n.d.). *NIBE F1155 Installer manual.* Retrieved from NIBE.com: https://www.nibe.eu/assets/documents/27897/331342-6.pd

REN21. (2021). Retrieved from https://www.ren21.net/why-is-renewable-energy-important/

Rivas, P. (2020). *GEOTHERMAL HEATING. RENEWABLE SOIL ENERGY*. Retrieved from instalacionesyeficienciaenergetica.com: https://instalacionesyeficienciaenergetica.com/geothermal-heating/

Rondina, R. (2020). ANALISI SPERIMENTALE DI UNA POMPA DI CALORE GEOTERMICA IN AMBITO RESIDENZIALE. *Tesi*, 12.

Tofalo, F. (2019). Sperimentazione di muri energetici. *Tesi di Laurea Magistrale*, 86.

Tofalo, F. (2019). *tesi "Sperimentazione di muri energetici".* Politecnico di Torino.

U. d. (2011). Guide to Geothermal heat pumps.

Wikipedia. (n.d.). *coefficient of performance*. Retrieved from https://en.wikipedia.org/wiki/Coefficient_of_performance